



# Late Cretaceous extension and exhumation of the Stong and Taku magmatic and metamorphic complexes, NE Peninsular Malaysia



T. François<sup>a,1,\*</sup>, M.A. Md Ali<sup>b</sup>, L. Matenco<sup>a</sup>, E. Willingshofer<sup>a</sup>, T.F. Ng<sup>b</sup>, N.I. Taib<sup>b</sup>, M.K. Shuib<sup>b</sup>

<sup>a</sup> Utrecht University, Faculty of Earth Sciences, Utrecht, The Netherlands

<sup>b</sup> University of Malaya, Faculty of Science, Kuala Lumpur, Malaysia

## ARTICLE INFO

### Keywords:

Post-orogenic extension  
Detachments  
Metamorphic core-complexes  
Syn-kinematic magmatism  
Peninsular Malaysia

## ABSTRACT

Fragmentation of large continental areas by post-orogenic extension requires favourable geodynamic conditions and frequently occurs along pre-existing suture zones or nappe contacts, as exemplified by the Stong and Taku magmatic and metamorphic complexes of northern Peninsular Malaysia. For this case, we have employed a field and microstructural kinematic study combined with low temperature thermo-chronology to analyse the tectonic and exhumation history. The results show that the Late Palaeozoic - Triassic Indosinian orogeny created successive phases of burial related metamorphism, shearing and contractional deformation. This orogenic structure was subsequently dismembered during a Cretaceous thermal event that culminated in the formation of a large scale Late Santonian - Early Maastrichtian extensional detachment, genetically associated with crustal melting, the emplacement of syn-kinematic plutons and widespread migmatization. The emplacement of these magmatic rocks led to an array of simultaneously formed structures that document deformation conditions over a wide temperature range, represented by amphibolite- and greenschist- facies mylonites and as well as brittle structures, such as cataclastic zones and normal faults that formed during exhumation in the footwall of the detachment. The formation of this detachment and a first phase of Late Cretaceous cooling was followed by renewed Eocene - Oligocene exhumation, as evidenced from our fission track ages. We infer that an initial Cretaceous thermal anomaly was responsible for the formation of an extensional gneiss dome associated with simple shear and rotation of normal faults. These Cretaceous processes played a critical role in the establishment of the presently observed crustal structure of Peninsular Malaysia.

## 1. Introduction

Large continental areas created by gradual accretion of continental and/or island arc elements are frequently fragmented and reorganized by later extensional episodes such as during continental rifting or the formation of new oceanic domains situated often in the back-arc of major subduction zones (Dewey, 1988; Doglioni et al., 2007; Hyndman et al., 2005; Ziegler and Cloetingh, 2004). The onset of such post-orogenic extension is commonly associated with large-scale transcurrent motions and the deposition of poorly-dated continental sediments that are spatially offset with respect to later marine depocentres (e.g., Aragon-Arreola and Martin-Barajas, 2007; Balázs et al., 2016; Prosser, 1993; Wernicke, 1992). Early structures are localized when compared with the subsequent development of large extensional systems and can be quantified only through integrated kinematic and thermo-chronological studies, as demonstrated for instance in the numerous continental extensional domes in the Mediterranean domain (e.g., Faccenna et al.,

2014; Jolivet et al., 2013; Vissers, 2012).

Understanding such evolution is important in SE Asia, where the Mesozoic and Early Cenozoic growth of the Sundaland continental mass, through convergence with Australian or Australia-derived terranes, was commonly followed by its extensional to transtensional dismembering (Hall, 2011; Hutchison, 1973c, 1989; Metcalfe, 2011). The Indosinian orogenic structure presently exposed west and north-west of the South China Sea in Thailand, Cambodia and Peninsular Malaysia formed in response to the Permian - Early Jurassic convergence and subduction of Paleotethys between the Australia-derived Sibumasu continent and the Indochina terrane (e.g., Hutchison, 1994; Metcalfe, 2013a; Morley et al., 2011). The accreted units comprise the Chantaburi-Sukhothai island arc (known also as the East Malaya Block), which is separated by its western and eastern continental units by the Bentong Raub - Inthanon and Sra Kao - Nan suture zones, respectively (Fig. 1a, e.g., Metcalfe, 2000; Sone and Metcalfe, 2008; Tan, 1996). The Late Cretaceous - Miocene evolution was characterized

\* Corresponding author at: Utrecht University, Faculty of Earth Sciences, PO Box 80021, 3508TA Utrecht, The Netherlands.

E-mail address: [thomas.francois@u-psud.fr](mailto:thomas.francois@u-psud.fr) (T. François).

<sup>1</sup> Present address: GEOPS, Université Paris-Sud, CNRS, Université Paris-Saclay, Rue du Belvédère, Bâtiment 504, F-91405 Orsay, France.

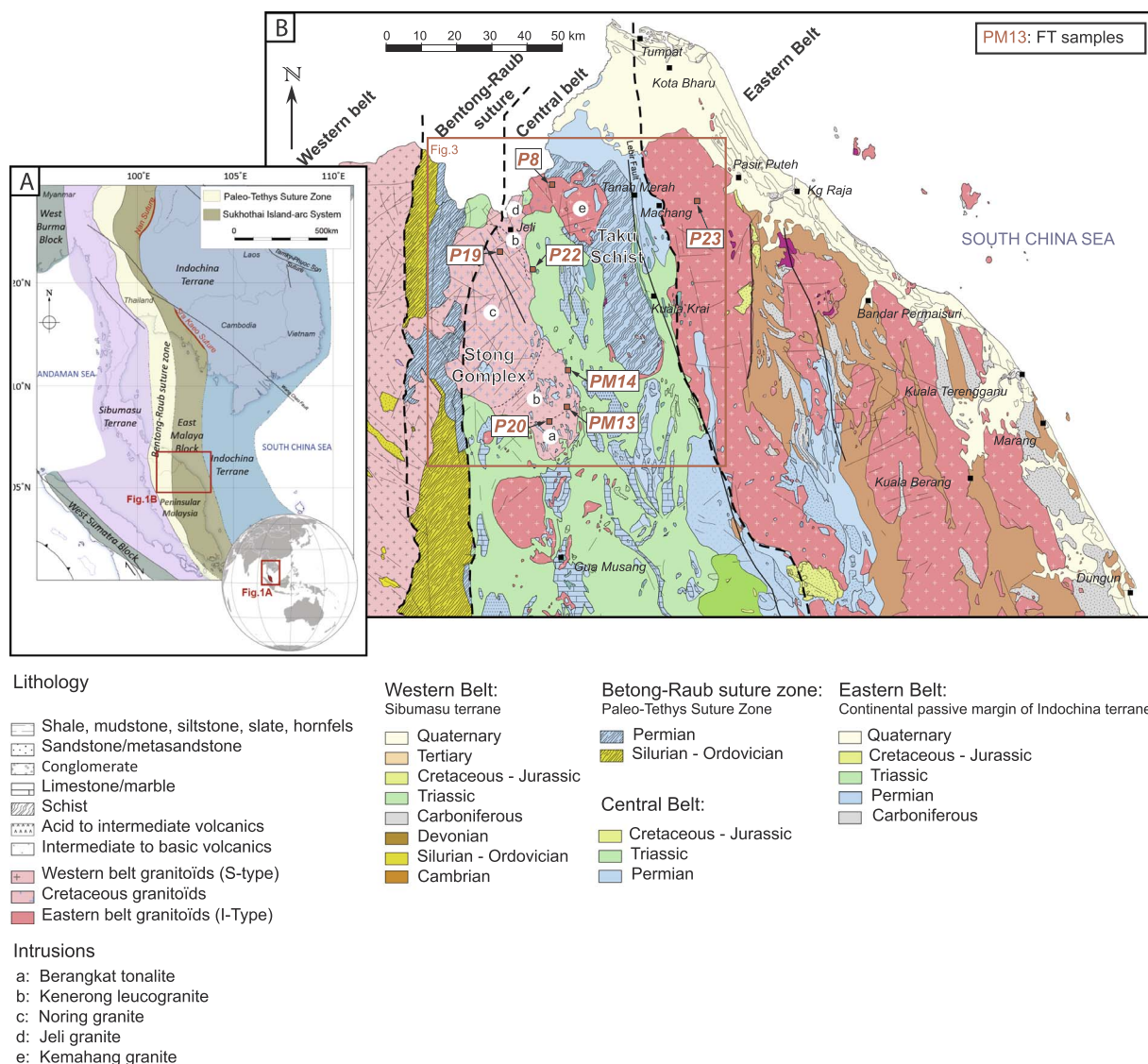


**Fig. 1.** (a) Simplified tectonic map of SE Asian continental units and suture zones. The Bentong–Raub suture zone separates the Sibumasu continental unit from the East Malaya Block (slightly modified after Metcalfe, 2013b). The red rectangle is the location of Fig. 1b; (b) the geological map of northern Peninsular Malaysia shows the Stong Complex and Taku Schist in the larger context of the Eastern, Central and Western Belts, and the Bentong–Raub suture zone (modified from Tate et al., 2008). It also shows available geochronological constraints (Bignell and Snelling, 1977a; Ng et al., 2015; Searle et al., 2012) and the location of the low-temperature thermo-chronology samples analysed in the present study. The rectangle is the location of Fig. 3. (For interpretation of the references to colour in this figure legend, the reader is referred to the web version of this article.)

by the formation of a significant number of localized strike-slip and extensional structures that predate or are coeval with the main opening of the South China Sea and the continuation or re-activation of subduction zones outside the orogen (e.g., Hall, 2012; Morley, 2012; Morley et al., 2011; Pubellier and Morley, 2014). For instance, reactivation of the Paleotethys suture zones in Thailand and Cambodia (Fig. 1a) created large extensional and transtensional structures, such as the Doi Inthanon core-complex (e.g., MacDonald et al., 1993; Morley et al., 2011). In this context, the kinematics and timing of potential reactivations of the Indosinian orogenic structure and genetically related Bentong–Raub suture zone in Peninsular Malaysia are particularly relevant (Hutchison, 2014; Hutchison and Tan, 2009; Tan, 1996; Tjia, 1994, 1996, 1998).

Although Late Cretaceous - Eocene deformations, including a Late Cretaceous thermo-tectonic event, can be inferred from folded Jurassic - Cretaceous strata and deformed Triassic granites, the kinematics, structure, thermo-chronological dating and regional significance of various structures in Peninsular Malaysia still require quantification (Cottam et al., 2013; Harun, 2002; Metcalfe, 2013b; Mustafa Kamal Shuib, 2000a,b; Ng, 1994; Tjia, 1996). In the north-east, the meta-

morphic and magmatic assemblages known as the Stong Complex (Hutchison, 2009) and Taku Schist (MacDonald, 1968) demonstrate Triassic and Late Cretaceous magmatism and migmatization as well as poly-phase deformation together with high-temperature contact and amphibolite-facies burial metamorphism (e.g., Ghani, 2009; Mustafa Kamal Shuib, 2009b). These are in strong contrast with the surrounding non-metamorphosed to lower greenschist-facies Palaeozoic - Triassic rocks of the Western and Central belts of Peninsular Malaysia (Fig. 1b, e.g., Hutchison, 2009; Metcalfe, 2013b). This contrast can be attributed likely to a Permo-Triassic orogenic burial, followed by a Late Cretaceous - Eocene exhumation along extensional detachments (e.g., Md Ali et al., 2016). However, both the timing of this exhumation phase, as well as the quantitative kinematics of the Stong Complex and the effects of the interplay between extension and strike-slip movements are relatively unknown.

We present an analysis of the structure, kinematics, conditions and sequence of deformation, and their relation to the metamorphism and cooling history of the Stong Complex and Taku Schist areas of NE Peninsular Malaysia. We do this by integrating low temperature thermo-chronology (zircon and apatite fission track dating) with field

and microstructural kinematic observations. Sparse outcrop exposures and the inferred grouping in the same regional structure requires the incorporation of the results described in our companion publication of Md Ali et al. (2016) in data description and interpretation. The results are discussed in terms of successive deformation and exhumation events, integration into regional structures and the mechanics of deformation.

## 2. The structure of the Stong and Taku magmatic and metamorphic complexes in the context of Peninsular Malaysia tectonic evolution

Peninsular Malaysia is traditionally subdivided in a Western Belt, Central Belt and Eastern Belt, separated by differences in magmatism, sedimentation, structure and, to a lesser extent, metamorphism (Fig. 1b, Foo, 1983; Ghani, 2009; Hutchison and Tan, 2009; Metcalfe, 2013b). The Western Belt forms part of the larger Sibumasu continental unit and is made up of Late Triassic - Early Jurassic S-type plutons intruded into a Cambrian - Triassic basement and (meta-)sedimentary sequence. In the vicinity of the plutons, the degree of contact metamorphism within the country rocks generally decreases towards their western and eastern flanks (Ghani, 2009; Hutchison, 1973a, 1977, 2009; Searle et al., 2012). The Central and Eastern Belts are part of the East Malaya block and are made up of Middle Permian to Late Triassic Sukhothai arc I-type plutons, which are associated with acid and basic volcanic rocks and are intruded into a Palaeozoic-Triassic fore- and intra- arc (meta-)sedimentary sequence (Ghani, 2009; Metcalfe, 2013b; Ng et al., 2015; Tan, 1984) (Fig. 2). The rocks are metamorphosed to various degrees, varying from sub-greenschist- to amphibolite- facies near the Triassic and Cretaceous intrusions, such as the Stong Complex, Taku Schist in the north, Benta Migmatite Complex in the centre and Gunung Ledang in the south (Fig. 1). These rocks recorded an interplay between contact and regional metamorphism during their evolution (Hutchison, 1973a, 1977, 2009; Khoo, 1980, 1983; Khoo and Lim, 1983; Kwan, 1990).

The Bentong-Raub Suture Zone contains remnants of the Paleotethys Ocean and was emplaced during Late Permian - Triassic subduction and collision of the Sukhothai continental unit with the East Malaya block (Metcalfe, 2000, 2013b). It is generally composed (Fig. 2) of a tectonic and sedimentary melange made up of deep water sediments containing large bodies of generally serpentinised mafic-ultramafic rocks, locally metamorphosed to greenschist-facies (e.g., Tiang Schist, Fig. 2), and has gradual or sharp structural transitions with neighbouring tectonic units (Hutchison, 1973a, 1975; Jasin, 2013; Setiawan and Abdullah, 2003; Metcalfe, 2000; Mustaffa Kamal Shuib, 2000b; Tan and Khoo, 1993; Tjia, 1984, 1987; Tjia and SImanshoor, 1996). The final emplacement of the suture zone was coeval with the deposition and deformation of a regressive Permian - Triassic foredeep sequence (Semanggol Formation) during the Indosinian collision (Baioumy and Ulfa, 2016; Harun et al., 2009; Jasin and Harun, 2007; Metcalfe, 2013b; Ridd, 2013).

The formation of the Permian-Triassic orogenic structure was followed by the widespread deposition of Jurassic - Cretaceous continental sediments (e.g., Fig. 2), generally interpreted to reflect the opening of a pull-apart basin along dextral strike-slip faults (Konjing et al., 2007; Madon et al., 2010; Mustaffa Kamal Shuib, 2009b; Nuraiteng Tee Abdullah, 2009). These sediments crop out mainly in the Central and Eastern belts, where they are folded and faulted by normal to sinistral strike-slip faults (Harbury et al., 1990; Mustaffa Kamal Shuib, 2000a,b; Tan, 1984; Tjia, 1996). Among such post-Indosinian structures, the Lebir Fault (Fig. 1) forms a diffuse gravity-defined transcurrent boundary between the Central and Eastern belts, the position of which changes along strike of the belt (Mustaffa Kamal Shuib, 2009b; Ryall, 1982; Tjia, 1969). Late Cretaceous magmatism is recorded in various areas of the Western and Central belts by intrusions and volcanic rocks, and is associated with significant contact metamorphism in adjacent sediments (e.g., Ghani, 2009; Ng et al., 2015; Searle et al., 2012 and

references therein).

In contrast to the numerous high-temperature formation and exhumation ages distributed all over the Peninsula, low-temperature exhumation data are scarce. A regional apatite and zircon fission track study of the Western Belt resulted in numerous Cretaceous - Eocene ages and demonstrated significant post-Indosinian cooling and/or tectonic exhumation (Krahenbuhl, 1991). A regional zircon and apatite U-Th-Sm/He and Ar-Ar thermo-chronological study showed significant ~ 100–90 Ma cooling followed by localized ~ 51–53 Ma exhumation, interpreted as an effect of a Cretaceous regional thermal perturbation followed by Paleogene regional transpression, compression and block faulting (Cottam et al., 2013). Previous studies have not been associated with quantitative field or micro- structural observations that allow of the discrimination of tectonic exhumation events quantified by low-temperature thermo-chronology.

### 2.1. The Stong Complex and Taku Schist

The Stong Complex in northern Peninsular Malaysia (Fig. 3) is composed of a complex system of migmatites injected into a magmatic and sedimentary complex affected by an upper greenschist- to amphibolite- facies metamorphism (the Stong Complex or the Stong Metamorphic Complex, Hutchison, 1969, 2009) situated in a multi-event plutonic system (Bignell and Snelling, 1977a; Ghani, 2009; Hutchison, 1969, 1973a, 2009; Searle et al., 2012). This multi-plutonic system includes the foliated and strongly deformed Triassic Berangkat pluton, the partly deformed Triassic Jeli granite, the deformed Late Cretaceous Kenerong leucogranite, and the un-deformed Late Cretaceous Noring granite (Fig. 3a, Bignell and Snelling, 1977b; Cobbing et al., 1992; Darbyshire, 1988). The upper Middle Triassic ( $231.8 \pm 1.7$  Ma, Ng et al., 2015) Berangkat pluton is a strongly foliated, coarse-grained monzonite - tonalite - granodiorite with large K-feldspars and meta-sedimentary enclaves or intercalations with shoshonitic composition (Ghani, 2009; Ng et al., 2015; Bacho and Umor, 2001; Singh et al., 1984; Umor et al., 2001). In the north, the Jeli granite is a complex fine to coarse-grained biotite granite intruded by basaltic dykes that display patterns of high-temperature deformation (Othman et al., 2000). Although the precise age is unknown, field relationships suggest that the granite is Triassic but may include local Cretaceous intrusions (Mustaffa Kamal Shuib, 2009a). The Kenerong intrusion is a deformed biotite leucogranite, characterized by a complex network of magmatic dykes with multiple generations of foliated fine to coarse-grained leucogranite veins and biotite granites, aprites and pegmatites, all intruded into a meta-pelitic sequence (Ghani, 2009; Jamin and Umor, 2001; Bacho and Umor, 2001). Xenoliths and enclaves/rafts of this amphibolite-facies meta-pelitic sequence contain a high temperature mineral assemblage that includes sillimanite and cordierite (Hutchison, 1973b; Singh et al., 1984). The Kenerong pluton has been dated by K/Ar biotite at  $69 \pm 2$  Ma (Bignell and Snelling, 1977a) and 65 Ma (Darbyshire, 1988), by whole rock Rb/Sr at  $79 \pm 3$  Ma (Cobbing et al., 1992), and recently by U-Pb at  $83.9 \pm 0.8$  Ma (Ng et al., 2015). The Noring granite, a large oval-shaped intrusion occupying the centre of the Stong Complex (Fig. 3), distinguished by its large K-feldspar phenocrysts, was emplaced at pressures of ~2–3 kbars and is usually separated into two facies by the presence/absence of hornblende (Terang and Belimbing, Tulot and Umor, 2001; Ghani, 2000a,b; Ghani, 2009; Jamin and Umor, 2001; Singh et al., 1984). It has been dated by K/Ar biotite at  $70 \pm 2$  Ma, by Rb/Sr biotite at  $66 \pm 1$  Ma and  $69 \pm 1$  Ma (Bignell and Snelling, 1977a) and recently by U-Pb zircon at  $75.7 \pm 0.6$  Ma (Ng et al., 2015).

The Kenerong and Noring intrusions are often associated with migmatitic textures that appear to relate to the assimilation of meta-sedimentary country rocks (Hutchison, 1969, 2009; Searle et al., 2012). Such structures may be observed in relatively small areas where the rock hosting the multi-event intrusion crops out and in numerous enclaves and rafts (Fig. 3). Previous studies have shown that this meta-



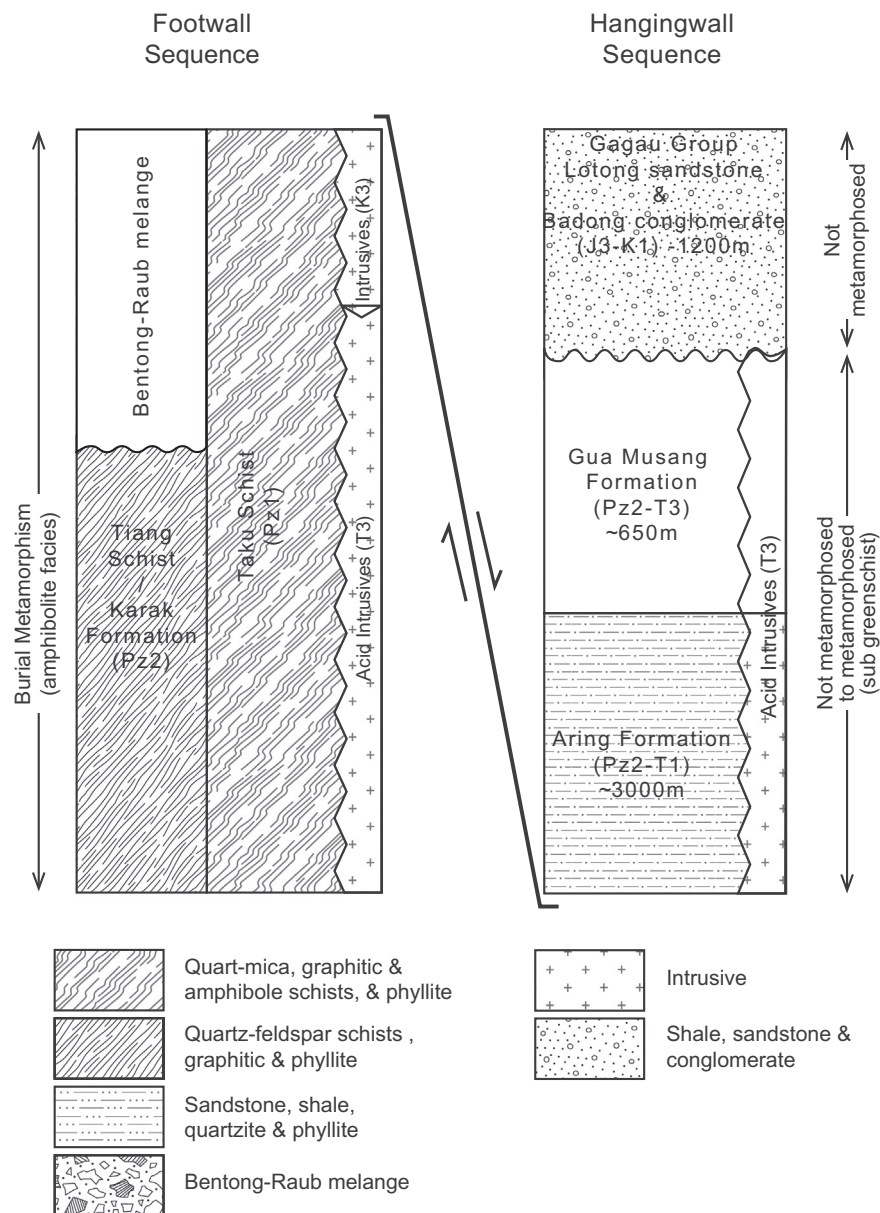


**Fig. 2.** Tectonostratigraphic columns of the two main units located in the northern part of Peninsular Malaysia, including the results of the present study. The footwall unit corresponds with the Taku Schist, Stong Complex and the adjacent area of the Western Belt including their Triassic and Late Cretaceous magmatic rocks, while the hanging-wall unit corresponds roughly with remaining areas of the Central and Eastern belts. Note the geometry of the extensional detachment between them depicted in Fig. 3 and further described in the text. The separation of these units in terms of metamorphic degree is less clear westwards (Fig. 3), where the offset of the extensional detachment decreases. Pz1 - Lower Palaeozoic, Pz2 - Upper Palaeozoic, P - Permian, T3 - Upper Triassic, J - Jurassic, K1 - Lower Cretaceous.

sedimentary sequence is diverse and can be described as meta-clastic with some intercalations of meta-carbonate and amphibolite (Hutchison, 2009; Abdullah and Setiawan, 2003; Singh et al., 1984). It contains hornblende-quartz schists, staurolite-garnet biotite schists, tourmaline bearing mica schists, diopside-phlogopite marbles, sillimanite-garnet-biotite gneiss and amphibolite. Three types of migmatites show transitions from isolated veins to mixed schist and magmatic material, while also showing spectacular ptygmatic folding, boudinage and intense buckling (Hutchison, 1969, 2009; Searle et al., 2012). Four phases of deformation have been proposed through field observations at the classical Renyok waterfall outcrop, which exposes the Kenerong granite and its high-temperature metamorphosed host rock sequence (6i,j in Fig. 3, Abdullah and Setiawan, 2003). Late Cretaceous foliation, isoclinal folding and veining took place during the emplacement of the intrusion and was followed by two phases of NW-SE contraction associated with boudinage, kink, ptygmatic and drag-folding, and

(later) normal faulting. Mylonites are intruded by at least three sets of leucogranite dykes, while three sets of deformed and boudinaged sills or dykes are parallel or cross-cut the foliation (Searle et al., 2012). It is unclear whether this post-magmatic emplacement resulted from stress-relaxation or from Cenozoic deformation (Abdullah and Setiawan, 2003; Mustafa Kamal Shuib, 2009b).

To the west (Figs. 1 and 3), the NNW-SSE elongated zone of meta-sediments composed dominantly of garnet-bearing quartz mica schists with narrow bands of quartz schist and quartz veins together with mafic bodies and meta-granitoids affected by amphibolite-facies metamorphism is widely known under the name of Taku Schist (Aw, 1974; Hutchison, 1973a; MacDonald, 1968). The metamorphic assemblage contains garnet (almandine), muscovite, biotite and kyanite, and has intercalations of calc-silicate metasomatic rocks, localized serpentinitic bands and amphibolite that are strongly foliated and sheared together in its entire mass (MacDonald, 1968). The amphibolite contains an

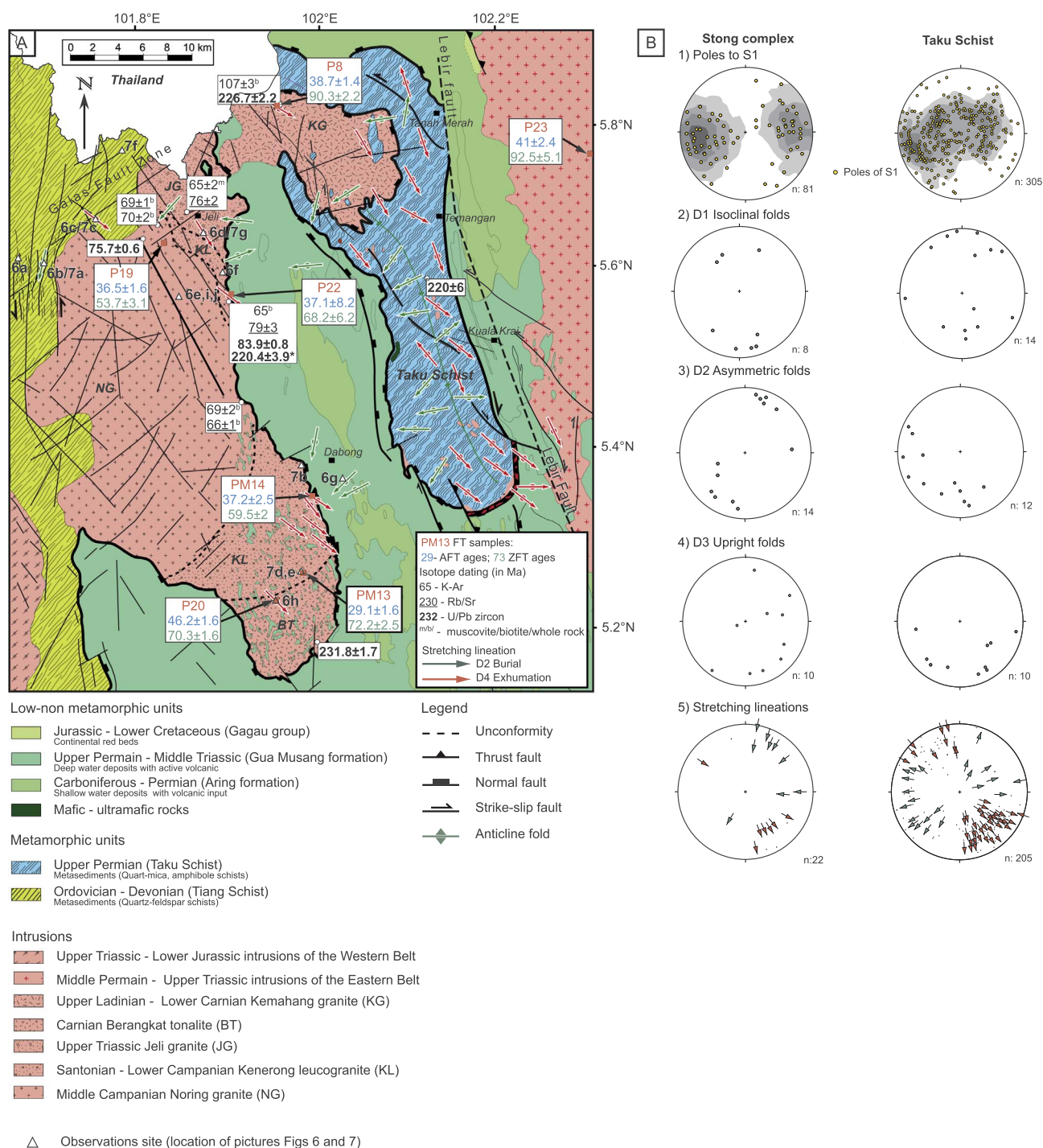


**Fig. 3.** (a) Detailed structural and geological map of the Strong Complex, Taku Schist and adjacent areas (after MacDonald, 1968; Md Ali et al., 2016) with geochronological constraints (Bignell and Snelling, 1977a; Darbyshire, 1988; Ng et al., 2015; Searle et al., 2012) and results of our low temperature thermo-chronology study, together with the senses of shear detected by the kinematic study. Green arrows indicate the direction of shearing related to nappe-stacking (D2) while red arrows indicate the direction of shearing related to exhumation (D5). Yellow triangles are locations of outcrop and microstructural photos depicted in Figs. 6 and 7; (b) stereoplots of foliations and kinematic structural data measured in the field. While the column for the Strong Complex results from the present study, the column for the Taku Schists shows the kinematic data of Md Ali et al. (2016). 1 - Stereoplots of the primary metamorphic foliation; 2 - Stereoplots of isoclinal folds F1 formed during the first deformation event D1; 3 - Stereoplots of asymmetric folds F2 formed during the second deformation event D2; 4 - Stereoplots of upright folds F3 formed during the third deformation event D3; 5 - Stereoplots of stretching lineations with the sense of shear: Green arrows show senses of shear formed during the second D2 deformation event, red arrows show senses of shear formed during the progressive D4 to D5 deformation events. (For interpretation of the references to colour in this figure legend, the reader is referred to the web version of this article.)

assemblage of hornblende, plagioclase, clinozoisite and epidote together with tremolite, garnet and biotite, while near the southern margin of the body interlayered bands of a meta-biotite granite (orthogneiss) crop out, often truncated by cataclastic shear zones with a sericite matrix (Hutchison, 1973a). Micro-structures show a fine-grained clastic protolith in which the main foliation is defined by

muscovite and quartz. Compositional bands associated with garnet formed during an initial burial metamorphism to amphibolite-facies. Top-W shearing associated with burial metamorphism contrasts with pervasive top-SE shearing related to exhumation accommodated along greenschist-facies mylonites deformed cataclastically during cooling (Md Ali et al., 2016). This study has shown that an initial phase of

burial and nappe stacking was followed by exhumation in the footwall of an extensional detachment, which likely exposed previously deeply buried Bentong-Raub Suture rocks. Available Late Triassic (~212–236) K-Ar biotite ages obtained for the Taku Schists (Bignell and Snelling, 1977b) probably reflect the initial burial, but the subsequent exhumation is thought to be Late Cretaceous - Eocene (Md Ali et al., 2016), although this remains to be confirmed.

In the northern part of the study area, the Triassic Kemahang granite ( $226.7 \pm 2.2$  Ma, Ng et al., 2015) apparently connects the structure of the Stong Complex and Taku Schist by intruding their dome-shaped structures (Figs. 1 and 3, Hutchison, 1973a,b; MacDonald, 1968). It extends northwards in southern Thailand, where is known as the Buke pluton (Cobbing et al., 1992). The foliation and shearing of the Kemahang granite is particularly obvious near its contact with the Taku Schists and Permo-Triassic sediments, where evidence for pre- to syn- kinematic emplacement and deformation relative to the initial Triassic burial metamorphism can be seen (Md Ali et al., 2016). Interestingly, U-Pb detrital zircons from present-day river sediments in the Taku Schist and Noring granite areas has resulted in mixed Late Triassic and Late Cretaceous ages (Sevastjanova et al., 2012).

The N-S oriented schists and phyllites observed in the western part of our study area (Fig. 1) are part of a longer belt of Ordovician, Silurian and Devonian sediments of the Bentong-Raub suture zone. This belt is thought to contain Sibumasu continental margin-slope deposits amalgamated into the accretionary wedge during subduction and metamorphism to greenschist-facies (Metcalfe, 2013b). In the western part of our study area, this belt is made up of foliated quartz-mica schists and phyllites with cordierite garnet schists and, locally, amphibolite containing actinolite and tremolite (Mustaffa Kamal Shuib, 2009b). In the study area, this belt is generally known as the Tiang Schist, which is a northward prolongation of the Lower Devonian Karak Formation (MGD, 2013). Owing to poor outcrops and difficult access, the detailed structure and kinematics of Tiang Schist is largely unknown in the study area.

The higher temperature metamorphosed sediments and plutonic rocks of the Stong Complex and Taku Schist are surrounded to the south, north and east by a non- to sub-greenschist facies metamorphosed Upper Palaeozoic - Triassic volcano-sedimentary sequence, Permo-Triassic plutons and Jurassic - Cretaceous continental sediments of the Central and Eastern Belt (Fig. 1). The Upper Palaeozoic - Triassic sediments of the Central Belt are generally ascribed to the Carboniferous - Triassic Raub Group (Alexander, 1959; Foo, 1983; Lee et al., 2014), which is composed of two formations, Gua Musang and Aring, including the Early Carboniferous to Middle Permian Kepis Beds (Khoo, 1998). The Upper Carboniferous - Lower Triassic Aring Formation (Foo, 1983; Lee, 2009) is dominated by pyroclastic rocks associated with lavas, dolomitic marbles, re-crystallized limestones and argillitic shales. The Middle Permian to Upper Triassic Gua Musang Formation (Lee, 2009; Lee et al., 2014; Mohd Shafeea Leman, 2004; Yin, 1965) starts with a basal conglomerate (the Gunong Ayam Conglomerate of Aw, 1974; Nuraiteng Tee Abdullah, 2009) and is composed dominantly of fissile shales with chert nodules associated with pyroclastic or acidic flows and acidic porphyritic lava, as well as with re-crystallized limestones and sandy sediments. The Gua Musang Formation is metamorphosed to sub-greenschist facies, as evidenced by the preferred alignment of sericite with cataclastic, zoned and strongly saussuritized relict feldspars (Khoo and Lim, 1983), and is affected by numerous structures formed during the E-W Indosinian shortening and subsequent normal faulting, (Md Ali et al., 2016). The upper part of the Gua Musang Formation laterally inter-fingers with carbonaceous shales, siltstones and volcanics of the Semantan Formation (Ismail et al., 2007; Lee, 2009; Madon, 2010; Nuraiteng Tee Abdullah, 2009; Umor et al., 2012), considered to represent the sediments, volcanics and volcanoclastics of a fore-arc basin deposited over the accretionary wedge situated at the margin of the Sukhothai arc (Hutchison, 1989; Metcalfe,

2000). In the study area, the Gua Musang Formation appears to become regressive and towards the top it is gradually replaced by a conglomeratic-sandstone sequence and terrestrial sediments (the Koh Formation of Aw, 1990; Nuraiteng Tee Abdullah, 2009). The affiliation of these latter clastics to the orogenic structure is unclear (Fig. 2). The formations described above are unconformably overlain by deformed Jurassic-Cretaceous continental sediments ("red-beds"), referred to in the Eastern Belt as the Gagau Group and separated into an older Badong Conglomerate and overlying Lotong Sandstone (Fig. 3, Nuraiteng Tee Abdullah, 2009). In the Central Belt, this generally fining upward sequence is affected by numerous km-scale folds and is composed, in the lower part, of conglomerates and sandstones associated with lava flows and pyroclastics (e.g., Konjing et al., 2007; Madon et al., 2010). These sediments crop out in large areas of the eastern part of the Central Belt and are significantly deformed along the diffuse and ill-defined Lebir Fault contact with the Eastern Belt (Figs. 1 and 3, Khoo and Lim, 1983; Mustaffa Kamal Shuib, 2009b; Tjia, 1969, 1996).

The character of the contact between the higher temperature metamorphosed sediments and plutonic rocks of the Stong Complex, Taku Schist and Tiang Schist with the sub greenschist-facies to non-metamorphosed Upper Carboniferous - Cretaceous sediments and magmatic rocks is not fully understood. What was previously interpreted as a conformable contact between the Taku Schist and adjacent rocks, and was assumed to involve a short lateral decrease (~5 km) in burial metamorphism (Hutchison, 2009; Khoo and Lim, 1983) has been proven to be represent a ductile to brittle shear zone associated with a post-orogenic detachment (Md Ali et al., 2016). There is an apparent decrease in metamorphic grade to greenschist-facies meta-sediments and amphibolite at the southern margins of the Stong Complex, while its margins are affected by cataclastic and brittle deformation (Hutchison, 2009; Abdullah and Setiawan, 2003; Singh et al., 1984).

### 3. Low-temperature zircon and apatite fission track thermochronology

Seven samples of granitic rocks were taken from key locations across the study area to correlate our low-temperature thermo-chronological study with existing higher temperature U/Pb zircon and/or Ar/Ar ages (Fig. 3). Six of the samples come from high temperature metamorphosed sediments and plutonic rocks of the Stong Complex and its northern Kemahang pluton prolongation, while one sample was taken from a granite intruding the sub-greenschist facies to non-metamorphosed sediments of the neighbouring Eastern Belt (Fig. 1b). One sample was taken from the Triassic Berangkat (P20), two samples from each of the Late Cretaceous Kenerong (PM13 and PM14) and Noring (P22 and P19), one sample came from each of the Triassic Kemahang (P8) and Nal-Terekak (~230 Ma, Ghani, 2009) intrusions (Fig. 3).

Apatite and zircon mineral separation, including crushing, sieving, heavy-liquid and magnetic separation followed standard procedures at VU Amsterdam, The Netherlands (e.g., Foeken, 2004; Stojadinovic et al., 2013). Apatite mounts were etched with 1.5 N HNO<sub>3</sub> at 21 °C for 35 s, while the zircons grain mounts were etched in a eutectic mixture of KOH and NaOH at 225 °C for 20–60 h. The etched mounts were attached against external mica detectors (EDM; Gleadow and Duddy, 1981) and irradiated at FRMII Garching (Technische Universität München, Germany). Zircon mounts were irradiated together with zircon age standards (Garver, 2003) and reference glass dosimeter CN-1, whereas apatite mounts were irradiated along with apatite age standards (Green, 1985) and reference glass dosimeter CN-5. Spontaneous and induced fission tracks were counted dry on a Leica optical microscope at a magnification of x1000 using an FTStage 4.04 (analyst Thomas François). Central ages (Galbraith and Laslett, 1993) have been calculated with the zeta calibration method (Hurford and Green, 1982), with a zeta-factor of  $355 \pm 11$  for the CN-5 glass (apatites) and  $170 \pm 6$  for the CN-1 glass (zircons). Dpar measurement was used to

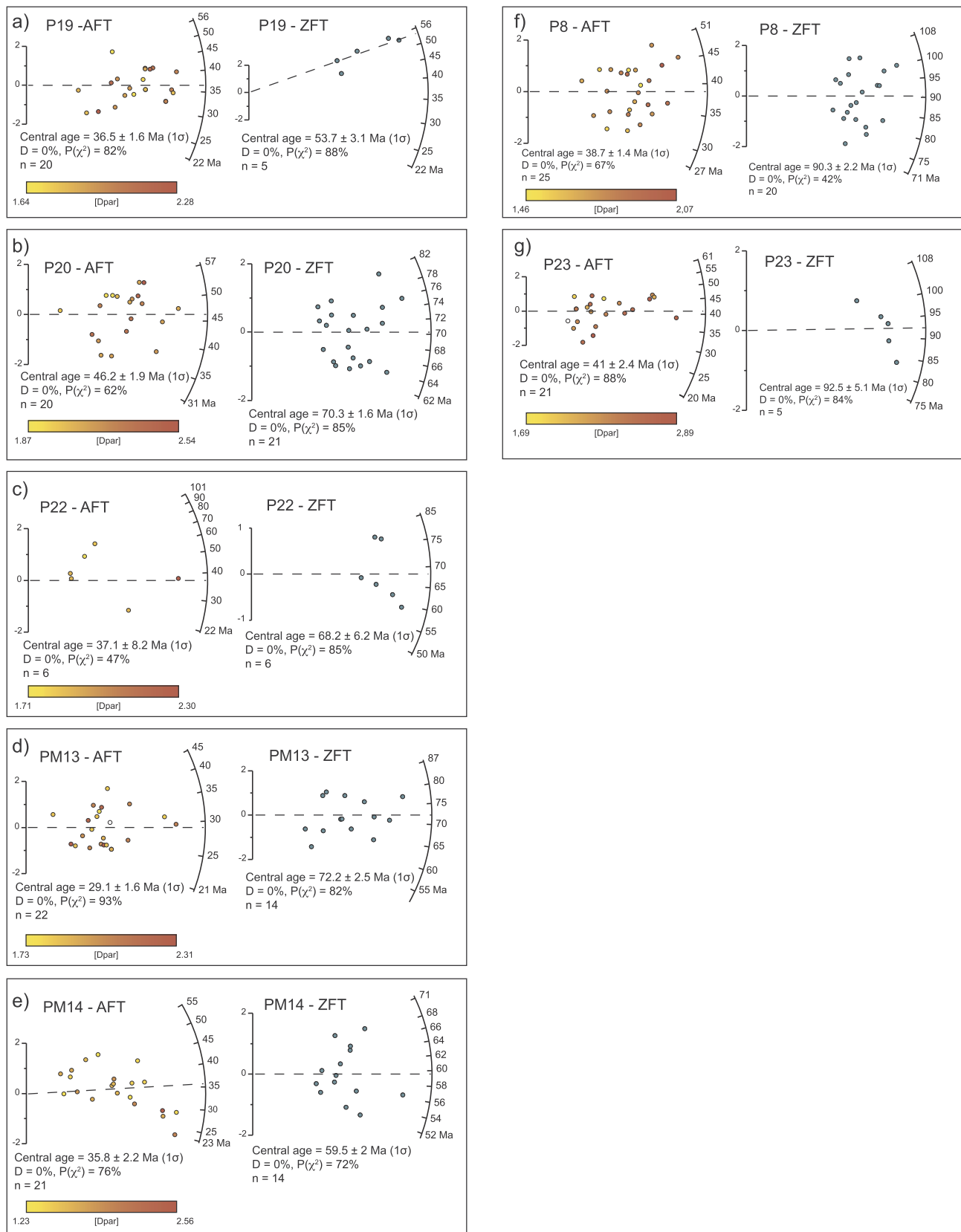


**Fig. 4.** Apatite and zircon fission track analytical results for samples collected in this study. For each sample, radial plots show single-grain ages. n - Number of analysed apatite and zircon grains. All samples passed the  $P(\chi^2)$  test > 5%. Dpar measurements were performed to characterize the chemical composition of the apatite crystals (Burtner et al., 1994). D = Dispersion. Error bars are in Ma with  $\pm 1$  sigma error. Further analytical results are available in Tables 1 and 2.



**Table 1**

Apatite fission track analytical data (see Galbraith and Laslett, 1993 for further details). The ages are calculated with 1 $\sigma$  standard error. Abbreviations  $\rho_s(N_s)$  = number of total spontaneous tracks,  $\rho_i(N_i)$  = number of total induced tracks,  $P(\chi^2)$  = chi-square probability ( $\chi^2$ ) for n degrees of freedom (n is the number of grains), Disp = dispersion in single-grain ages.

Sample	No of grains	$\rho_s(N_s) \times 10^5 \text{ cm}^{-2}$	$\rho_i(N_i) \times 10^5 \text{ cm}^{-2}$	$P(\chi^2)$ (%)	Disp (%)	Central age (Ma)	1 $\sigma$ (Ma)
P8	25	936	2390	67	0	38.7	1.4
P19	20	648	3588	82	0	36.5	1.6
P20	20	755	3300	62	0	46.2	1.9
P22	6	24	131	47	0	37.1	8.2
P23	21	365	1804	86	0	41	2.4
PM13	22	380	2657	93	0	29.1	1.6
PM 14	21	299	1668	50	12	37.2	2.6

**Table 2**

Zircon fission track analytical data (see Galbraith and Laslett, 1993 for further details). The central ages are calculated with 1 $\sigma$  standard error. Abbreviations  $\rho_s(N_s)$  = number of total spontaneous tracks,  $\rho_i(N_i)$  = number of total induced tracks,  $P(\chi^2)$  = chi-square probability ( $\chi^2$ ) for n degrees of freedom (n is the number of grains), Disp = dispersion in single-grain ages.

Sample	No of grains	$\rho_s(N_s) \times 10^5 \text{ cm}^{-2}$	$\rho_i(N_i) \times 10^5 \text{ cm}^{-2}$	$P(\chi^2)$ (%)	Disp (%)	Central age (Ma)	1 $\sigma$ (Ma)
P8	20	5464	2439	42	0	90.3	2.2
P19	5	714	533	88	0	53.7	3.1
P20	21	5309	2906	41	3.5	70.3	1.6
P22	6	302	194	100	0	68.2	6.2
P23	5	1075	471	82	0	92.5	5.1
PM13	14	2405	1276	93	0	72.2	2.5
PM 14	14	2374	1499	72	0	59.5	2

characterize the chemical composition of the apatite crystals (Burtner et al., 1994). To analyse the homogeneity of the single-grain ages per sample the Chi-square ( $\chi^2$ ) test was used, which returns the probability ( $P(\chi^2)$ ) that the single-grain ages are derived from the same population. When a  $P(\chi^2) > 5\%$  is obtained, the sample passes the chi-square test and, therefore, the age population is considered to be homogeneous (Barbarand et al., 2003; Bernet and Spiegel, 2004). Zircon fission tracks (ZFT) and apatite fission tracks (AFT) results are available in Fig. 4, Tables 1 and 2. All samples passed this chi-square test with a  $P(\chi^2) > 5\%$  indicating a single cooling age distribution for each sample, with no indication of partial resetting. Therefore, the populations are homogeneous (Brandon, 1992; Galbraith, 1981). These ages are further discussed in the text as central ages with  $\pm 1\sigma$  uncertainties (Galbraith and Laslett, 1993). These fission track ages were calculated with *RadialPlotter* software (Fig. 4, Vermeesch, 2009).

To constrain the cooling trajectories for different samples, the thermal history was modelled by using the QTQt approach that allows a Markov chain Monte Carlo (MCMC) approach (Gallagher, 2012; Gallagher et al., 2009). The samples' thermal history was constrained by the fission track ages and existing geochronology data including U/Pb, Rb/Sr and K/Ar age from Stong Complex and Kemahang granite correlated with the northern Buke pluton and Eastern Belt granites (Fig. 5). The low amount of confined fission tracks was not sufficient for the statistical analysis of track length measurements.

### 3.1. Fission tracks results

AFT central ages range from  $46.2 \pm 1.9$  Ma to  $29.1 \pm 1.6$  Ma in the studied samples (Figs. 3a and 4, Table 1). The AFT central ages obtained for the Stong Complex are Eocene-Oligocene in age, ranging from  $36.5 \pm 1.6$  Ma (sample P19, Noring granite),  $37.1 \pm 8.2$  Ma (sample P22, Kenerong leucogranite),  $37.2 \pm 2.6$  Ma (sample PM14, Kenerong leucogranite),  $29.1 \pm 1.6$  Ma (PM13, Kenerong leucogranite) to  $46.2 \pm 1.9$  Ma (sample P20, Berangkat tonalite). The sample from the Kemahang granite (P8) resulted in an Eocene AFT age of  $38.7 \pm 1.4$  Ma, while the sample from the Nal-Terekak (P23) granite resulted in an Eocene AFT age of  $41 \pm 2.4$  Ma.

ZFT central ages range from  $92.5 \pm 5.1$  Ma to  $53.7 \pm 3.1$  Ma in the studied samples (Figs. 3a and 4, Table 2). The ZFT ages obtained for

the Stong Complex are latest Campanian - Paleocene, ranging from  $53.7 \pm 3.1$  Ma (sample P19, Noring granite),  $68.2 \pm 6.2$  Ma (sample P22, Kenerong leucogranite),  $59.5 \pm 2$  Ma (sample PM14, Kenerong leucogranite),  $72.2 \pm 2.5$  Ma (sample PM13, Kenerong leucogranite) and  $70.3 \pm 1.6$  Ma (sample P20, Berangkat tonalite). The sample from the Kemahang granite (P8) resulted in a Turonian ZFT age of  $90.3 \pm 2.2$  Ma, while the sample from the Nal-Terekak granite (P23) resulted in a Late Cenomanian - earliest Coniacian ZFT age of  $92.5 \pm 5.1$  Ma.

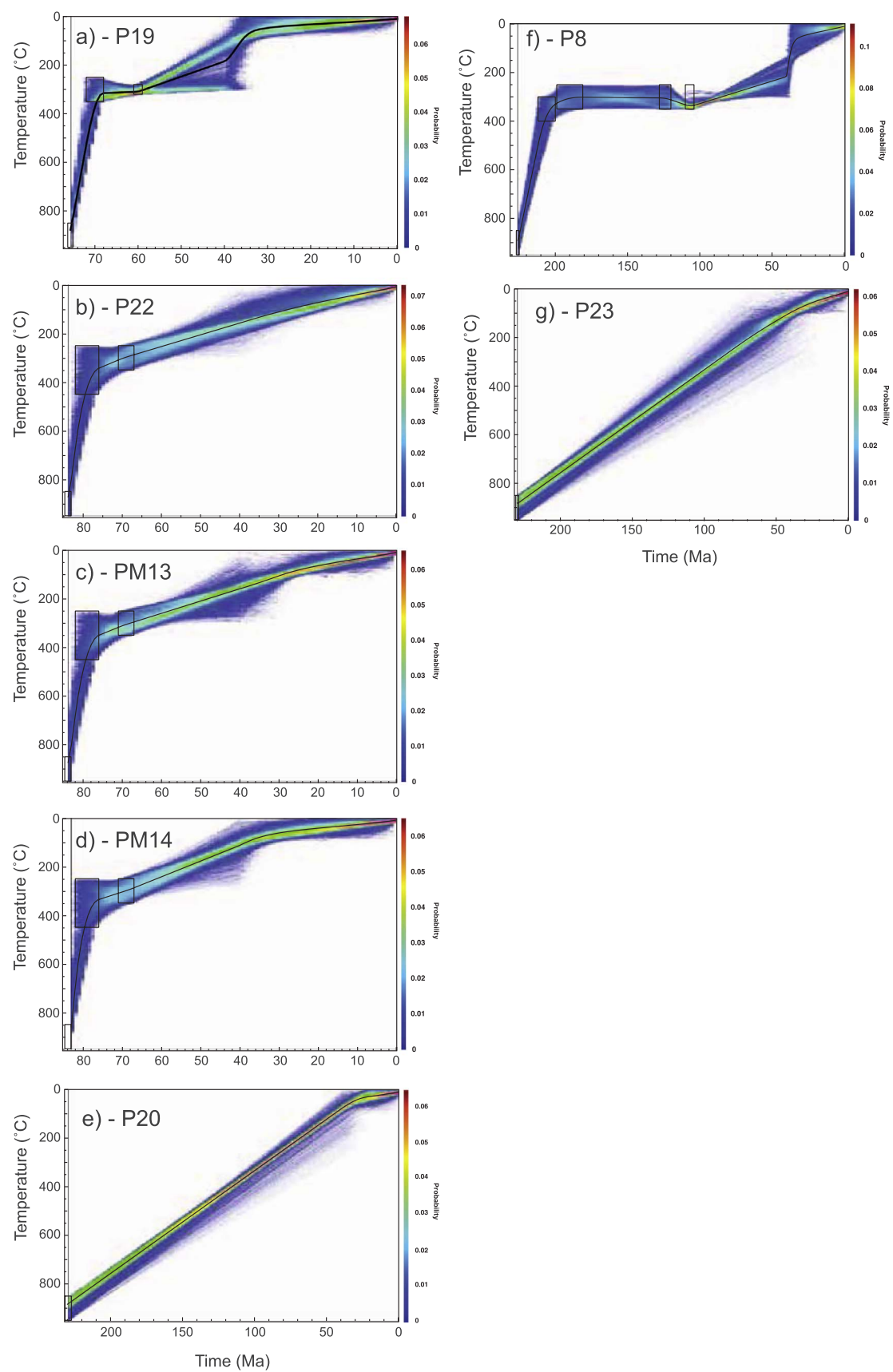
The QTQt modelling demonstrates accelerated exhumation of the Kenerong leucogranite during the Late Cretaceous, possibly continuing during the Paleogene (Fig. 5b–d), it implies a wide latest Cretaceous - Paleogene rapid exhumation of the Noring granite (Fig. 5a) and rapid Late Cretaceous - Early Paleogene exhumation of the Berangkat tonalite (Fig. 5e). It also indicates a widespread Late Cretaceous - Paleogene accelerated exhumation for the Kemahang granite (Fig. 5f). Outside the Stong Complex and Taku Schist area, the modelling shows gradual cooling throughout Cretaceous and Paleogene times (Fig. 5g).

### 4. Field kinematic and microstructural data

Field kinematic and micro-structural observations included measurements of ductile and brittle planar structures such as penetrative and mylonitic foliations, axial plane cleavages, fault planes and cataclastic shears and fault gouges. Measured linear structures include stretching lineations, fold axes or slickensides. Brittle slickensides and Riedel shears together with ductile kinematic indicators in shear zones, such as shear bands or sigma clasts, were used to derive the tectonic transport in various units. These observations were generally grouped into deformation events (Fig. 3) and exemplified in representative outcrops (Fig. 6). Superposition criteria, such as the evolution of the metamorphic facies, stratigraphic constraints, overprinted mineral associations, truncations, tilting and post-kinematic deposition were used wherever possible to derive the relative or absolute timing of deformation. The microstructural observations were used to define the metamorphic facies associations and to study the kinematics of deformation in detail (Fig. 7).

The low amount of field measurements is linked to the extreme scarcity and quality of outcrops. This was partly compensated by a





(caption on next page)

**Fig. 5.** Time-temperature history of samples analysed in the present study by using AFT and ZFT ages (Fig. 4) combined with existing absolute age constraints available from existing studies in their vicinity (black boxes). The latter are 65 Ma K-Ar muscovite age,  $69 \pm 2$  Ma K-Ar biotite,  $79 \pm 3$  Ma whole rock Rb/Sr age,  $83.9 \pm 0.8$  Ma zircon U/Pb age in the Kenerong granite in samples P22, PM13 and PM14 (Cobbing et al., 1992; Darbyshire, 1988; Ng et al., 2015);  $70 \pm 2$  Ma K-Ar biotite,  $66 \pm 1$  Ma and  $69 \pm 1$  Ma Rb/Sr biotite,  $75.7 \pm 0.6$  Ma zircon U/Pb age in the Noring granite in sample P19 (Bignell and Snelling, 1977a; Ng et al., 2015);  $107 \pm 3$  Ma K-Ar biotite age,  $226.7 \pm 2.2$  Ma zircon U/Pb age in the Kemahang granite in sample P8 (Bignell and Snelling, 1977a; Ng et al., 2015);  $231.8 \pm 1.7$  Ma zircon U/Pb age in the Berangkat tonalite in sample P20;  $107 \pm 3$  Ma K-Ar biotite,  $226.7 \pm 2.2$  Ma zircon U/Pb in the Kemahang granite combined with  $124 \pm 4$  and  $190 \pm 9$  K-Ar biotite and  $206 \pm 6$  K-Ar muscovite ages in the continuation of the Buke granite in Thailand (Bignell and Snelling, 1977a; Hughes and Bateson, 1967; Ishihara et al., 1980; Ng et al., 2015) in sample P8;  $\sim 230$  Ma zircon U/Pb in the Triassic Nal-Terekak in sample P23 (Ghani, 2009). Note that track length measurements were not performed due to the limited availability of AFT samples. The colour bar represents the probability of the best fit represented by the black line (expected model), as being the 95% credible intervals.

higher number of micro-structural observations. Using a quantitative kinematic analysis, we have re-evaluated outcrops described by previous authors, such as at the Renyok waterfall (Hutchison, 2009; Abdullah and Setiawan, 2003; Searle et al., 2012). The results are compatible and are discussed together with the results of the kinematic analysis available in the Taku Schist area in our companion study of Md Ali et al. (2016) (Fig. 3b, right column).

In summary, the overall deformation history described below includes a succession of orogenic shortening, magmatism and metamorphism (D1, D2 and D3). This orogenic shortening was overprinted by subsequent magmatism, contact metamorphism and deformation during exhumation (D4) (Figs. 3, 6 and 7).

#### 4.1. Initial burial, metamorphism, shearing and contraction (D1–D3)

The Stong Complex, Taku Schist and neighbouring areas were affected by an initial stage of burial metamorphism, shearing and contractional deformation. This deformation is observed both in the high temperature metamorphosed rocks of the Stong Complex and Taku Schist that predate the Late Cretaceous magmatism as well as in the Gua Musang and Aring formations.

A primary metamorphic foliation (S1) is associated with the formation of the initial metamorphic paragenesis. This foliation is associated with metamorphism from upper greenschist- to amphibolite-facies in the Stong meta-sedimentary sequence, Kemahang granite and parts of the Berangkat tonalite, decreasing to greenschist-facies in the Tiang Schist. The S1 foliation was subsequently affected by Late Cretaceous contact metamorphism associated with the pluton emplacement, as observed at the Renyok waterfall (see also Hutchison, 2009; Searle et al., 2012), where a relict foliation is affected by subsequent metasomatic growth of higher temperature minerals, such as garnet or sillimanite. In Tiang Schist areas less affected by the subsequent metamorphism, the penetrative foliation (S1) formed by the transposition of an initial bedding and was associated with isoclinal folding (F1, Fig. 6a). Locally, the original bedding is oblique to the flattening direction, resulting in deviations in the orientation between the primary foliation and the axial plane of the isoclinal folds. This primary foliation generally dips eastwards and westwards in the Stong Complex by forming an antiformal structure (Fig. 6b). The foliation dips steeply in the Gua Musang formation and has a general westward vergence. The isoclinal folds have generally N-S oriented hinges that plunge towards the north and south along the structure of the antiformal Stong Complex. We observed isoclinal folds in outcrops at cm- to metre scale (Fig. 6a) through the folding of quartz-feldspatic layers in which the quartz migrated to the hinges of the isoclinal folds by dissolution and precipitation creep (e.g., Cox and Paterson, 1991; Rutter and Elliott, 1976). In thin sections, S1 is defined by fine-grained muscovite and biotite (Fig. 7a), which together with quartz define the main metamorphic paragenesis. A difference in grain size is observed across the Stong Complex, with larger size in the east and decreasing westwards (compare Fig. 7a and b). This may point to higher temperatures in the east during the initial metamorphism.

The initial foliation was followed by top-SW shearing, asymmetric folding and rare thrust faulting (D2, Fig. 3). Similar with the first phase of burial, prograde metamorphism continues and reaches greenschist- to amphibolite-facies in the Stong Complex, Tiang Schist and Taku

Schist, while the deformation is mostly brittle in the Gua Musang and Aring formations. This contrast was created by phases of exhumation of the higher temperature metamorphic rocks. Often asymmetric folds can be observed in the northern part of the Tiang Schist, west of the Stong Complex (Fig. 6b and c), where metre to centimetre scale folds can be observed in densely foliated schistose lithologies. These folds can also be observed in the higher amphibolite-facies that characterize the orthogneisses of the Stong Complex (Fig. 6d). As in the Taku Schist, the asymmetric folds have dispersed axial planes orientation, but trend generally SW-NE, although the number of such measured folds is quite limited in the Stong Complex area (Fig. 3b). The second phase of deformation was also associated with shearing, mylonitisation and the formation of a clear stretching lineation, as observed in the meta-sediments intruded by the Kenerong leucogranite (e.g., at the Renyok waterfall, Fig. 6e), or in meta-sediments near the contact with the intruding Noring granite (Lata Tubur, Fig. 6f). Field kinematic indicators are generally shear-bands (Fig. 6f) and sigma clasts indicating a dominantly top to SW-SSW sense of shear. The degree of metamorphism during this shearing phase decreases to the west in the Tiang Schist, where S-C fabrics formed under semi-brittle conditions. This deformation event was also associated with the formation of rarely observed reverse faults and high-angle transpressive faults in the Gua Musang and Aring formations. The latter are, however, more clear near the Taku Schist area. In thin sections, the primary foliation within schists consists of bands of muscovite or biotite and that of gneisses or foliated granites was subsequently affected by shear bands that indicate top-SW-SSW sense of shear (e.g., D2, Fig. 7a). This is more obvious at greater distances from the Late Cretaceous plutons, such as in the Tiang Schist, where the later metasomatic mineral growth is limited or absent.

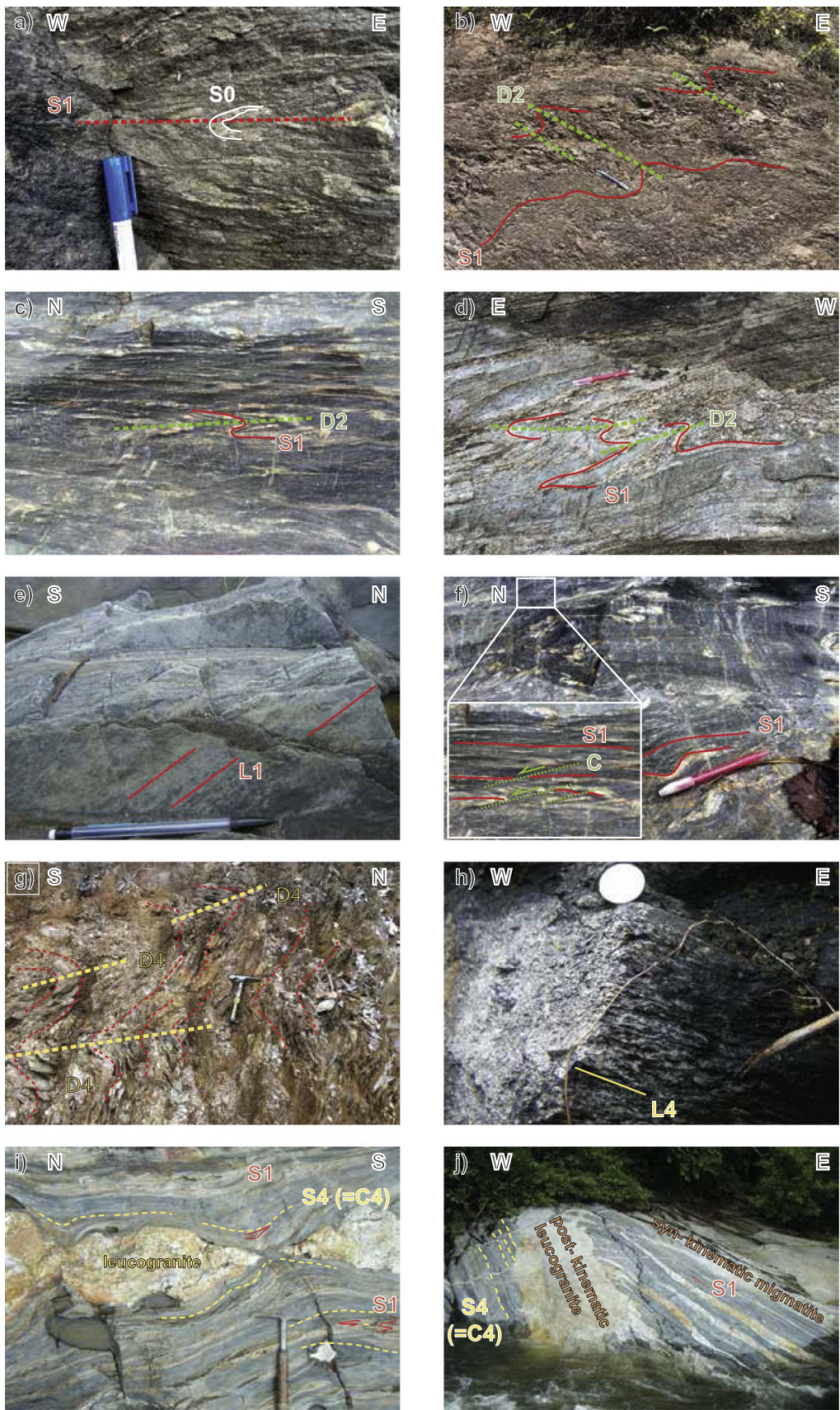
The shearing was followed by a subsequent phase of contraction characterized by the formation of open and upright symmetrical folds (D3, Fig. 3b). These folds are generally metre-scale in outcrop and affect all earlier burial and contraction structures. Their size and geometry is significantly different when compared with the subsequent kilometre-scale folding affecting the Jurassic - Cretaceous red-beds. The orientation of their hinges is spread, but a general N-S trend can be inferred.

#### 4.2. Magmatism, contact metamorphism, migmatitisation and deformation during Cretaceous to Eocene exhumation (D4)

The study area was affected by contact metamorphism and migmatitisation during the Late Cretaceous magmatism. The deformation affected the Taku Schist and Stong Complex, including the marginal areas of the undeformed Noring granite. Observed deformation (D4) includes brittle and ductile structures, documenting top-SE shearing associated with folds showing sub-horizontal axial planes. All these structures affect the Taku Schist and all Stong Complex units except for the main mass of the Noring granite and rocks associated with the last episode of migmatite emplacement (Fig. 3).

The shearing was pervasive in the Taku Schist and in the SE marginal areas of the Stong Complex (Fig. 3). In outcrop, ductile D4 structures include a mylonitic foliation containing stretching lineations associated with sigma-clasts and shear-band geometries. Deformation in the Taku Schist is associated with a pervasive stretching lineation observed in the entire unit with consistent top-SE sense of shear (Fig. 3). Shearing was more intense in the marginal areas, forming mylonitic





(caption on next page)



**Fig. 6.** Field kinematics examples; locations are displayed in Fig. 3. (a) Example of F1 isoclinal fold in quartz-feldspar schist in the Tiang Schist in the NW part of the Stong Complex; (b) example of D2 asymmetric folding in the Tiang Schist in the NW part of the Stong Complex; (c) asymmetric D2 folding in the Tiang Schist in the NW part of the Stong Complex (Laba Tubur); (d) asymmetric D2 folding in orthogneisses in the northern part of the Stong Complex; (e) example of F1 stretching lineations associated with D2 burial in a metasedimentary rock (quartzo-feldspathic schists) near the contact with the Kenerong leucogranite; (f) S-C shear bands fabric formed during the D2 deformation event in the NNW part of the Stong Complex (Laba Tubur) near the contact between with the intruding Noring granite; (g) example of F4 folds with sub-horizontal axial planes formed during the extensional event in phyllites situated within the Gua Musang formation near the eastern margin of the Stong Complex; (h) example of shear bands and sigma clasts associated with D4 high temperature stretching in orthogneisses. These orthogneisses are in fact sheared Triassic Berangkat granites near the limit with the neighbouring Gua Musang Formation; (i) meta-sedimentary quartzo-feldspathic rock that contains foliated and boudinaged Late Cretaceous Kenerong migmatite at the Renyok waterfall site. This demonstrates that the last high-temperature contact metamorphic foliation parallel with the elongation of the boudins formed during the D4 Late Cretaceous high-temperature event; (j) relationship between syn- to post- kinematic magmatic veins emplaced during and after the Late Cretaceous high-temperature event. Magmatic veins elongated in the direction of the last foliation are cross-cut by later veins of the same magmatic event.

leucogranite and micaschist zones that were subsequently truncated by more cataclastic, brittle normal and dextral strike-slip faults with the same sense of shear at the contact with or in the Gua Musang and Aring formations (see Md Ali et al., 2016 for further details).

In the Stong Complex, D4 shearing is more obvious and is associated with retrograde metamorphism observed by grain-size reduction and the formation of sericite and chlorite in shear zones away from the Noring granite and related migmatites. The Kenerong leucogranite was affected by pervasive shearing that displays grain-size reduction with the formation of sericite and chlorite (e.g., Fig. 7g). In meta-sediments that were affected by a high degree of migmatization or are located adjacent to the Noring or Kenerong plutons, the shearing is observed as a fine stretching lineation affected by and cross-cutting metasomatic zones, while kinematic indicators are less obvious due to plasticity of clasts (e.g., feldspars) deformed at higher temperatures. In these latter areas, the observed pervasive D4 foliation formed from high-temperature C shear planes associated with significant co-axial flattening that affected all previous structures and boudinaged the earlier emplaced leucogranite or migmatitic veins or sills. This is obvious for instance at the Renyok waterfall, where shearing, co-axial flattening and boudinage affects pre-existing isoclinal or asymmetric folds (i.e. deformation phase D2) (Fig. 6i). Multiple generations of veins and sills with leucogranitic composition (Fig. 6j, see also Searle et al., 2012) were clearly formed from a migmatitic leucosome injected into the host meta-sediments, as previously noted by Hutchison (2009). These amphibolite-facies meta-sediments form a thick mylonitic zone created by the high temperature of the neighbouring plutons and injected migmatites that were emplaced during and after deformation (Fig. 6i and j). Although still visible, the stretching lineations are strongly overprinted by the almost coeval high-temperature quartzo-feldspathic flow and metasomatic growth of various minerals, such as hornblende, andalusite or sillimanite. The deformation is also associated with the formation of decimetre to metre scale folds with sub-horizontal axial planes affecting inherited steep foliations or previous folds in the lower grade metamorphics of the Tiang Schist and Gua Musang Formation (Fig. 6g, collapse folds, sensu Froitzheim et al., 1997). The contact between the Stong Complex and the neighbouring Gua Musang and Aring formations is always tectonic, as can be observed by the mylonitic fabric, or by the fact that the Noring pluton is truncated by cataclastic shear zones or brittle normal faults. These normal faults have the same top-SE kinematics as the mylonites and formed most probably during later stages of cooling and/or exhumation. The marginal areas of the Noring pluton show also a similarly oriented but less marked foliation associated with brittle shears, although this was difficult to quantify in the field.

In thin sections, samples from the Stong Complex show a D1 fabric that is strongly overprinted by a high temperature contact metamorphism in the vicinity of the Late Cretaceous plutons and injected migmatites. This metamorphism results in coarsening of the rock and the growth of porphyroblasts including andalusite and sillimanite in meta-pelitic and hornblende in meta-volcanic rocks. In the latter rocks, the hornblende grows obliquely over the penetrative foliation S1 (Fig. 7c). In meta-pelitic rocks the metamorphic paragenesis consists of muscovite, biotite and andalusite (Fig. 7f and g) or sillimanite, together with K-feldspar, subordinate plagioclase, quartz and rare

garnet (Fig. 7d and e). Quartz rich domains in these rocks are typically characterized by straight grain boundaries. Sillimanite is strongly intergrown with biotite and is aligned parallel to the shear planes (Fig. 7e). The high temperature shearing is evidenced by asymmetric porphyroblasts associated with K-feldspar growing in the strain shadow of a large biotite porphyroblast (Fig. 7e). Sillimanite wraps around porphyroblasts or is isoclinally folded, indicating significant flattening of the rock after the growth of the porphyroblast (Fig. 7e). This is also observed where foliations defined by fine-grained muscovite and biotite wrap around andalusite porphyroblasts (Fig. 7f). This high-temperature fabric was overprinted by low-temperature deformation, which led to the fracture of andalusite, garnet and feldspar porphyroblasts and the development of shear bands (Fig. 7d and g). Shear band formation is associated with the replacement of biotite by chlorite, which grows along C' planes (Fig. 7g). Both high and low-temperature shearing show top-SE sense of tectonic transport. Field and microstructural evidence suggest that these events, i.e. high-temperature magmatism, metasomatism and deformation followed by low-temperature deformation, were continuous. Deformation started at high-temperature during migmatization (e.g., Fig. 7e) and continued during cooling and retrograde metamorphism, when the biotite was partly replaced by chlorite and porphyroblasts were affected by semi-brittle deformation (e.g., Fig. 7g).

## 5. Interpretation

Our field and microstructural observations combined with thermochronological data from the Stong Complex - Taku Schist and neighbouring Tiang Schist, Gua Musang and Aring formations clarify the Late Cretaceous deformation mechanics and allow more precise timing. The structural interpretation was aided by the time-temperature evolution of the main tectonic units in the study area (Fig. 8) calibrated against existing U-Pb zircon ages of the Berangkat, Kenerong, Noring and Kemahang plutons (Fig. 3, Ng et al., 2015; Searle et al., 2012). This calibration was correlated with the Rb-Sr ages (whole rock, biotite or muscovite, Bignell and Snelling, 1977a,b; MacDonald, 1968), although the error bars in their time-temperature history are quite large (Fig. 8). Revising the available K-Ar data shows that a significant number of ages are derived from micas with low K concentrations, which casts some doubt on their reliability. Therefore, we did not make use of the samples of Bignell and Snelling (1977a) in the time-temperature interpretation (Fig. 8), although their inclusion would not have changed the interpretation significantly. Furthermore, one of the numerous schist xenoliths observed in the Kemahang granite has been dated by K-Ar biotite at  $107 \pm 3$  Ma (Bignell and Snelling, 1977a), which is significantly younger than the U-Pb zircon Triassic age of the pluton ( $226.7 \pm 2.2$  Ma, Ng et al., 2015). Such apparently conflicting ages are probably the result of polyphase tectonic deformation and metamorphism during and after the main phase of plutonic emplacement (see discussion in Hutchison, 1973a,b; Khoo, 1980; Md Ali et al., 2016) and, therefore, the K-Ar age should be treated with caution.

### 5.1. Indosinian nappe stacking and late stage deformation

The Indosinian orogenic build-up created by convergence between

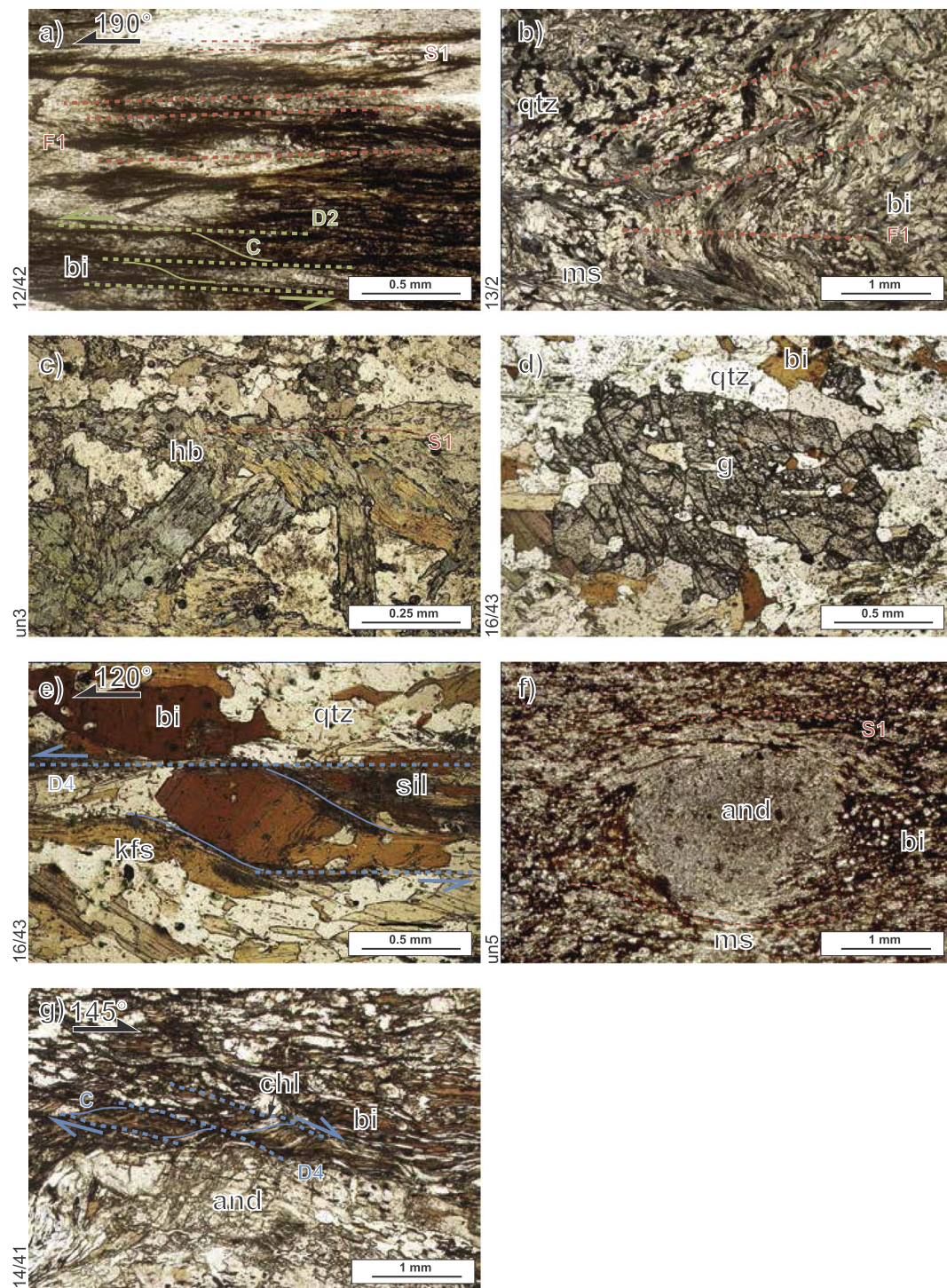


**Fig. 7.** Examples of microstructural observations in the Stong Complex and surrounding areas. Locations are displayed in Fig. 3. (a) A fine-grained white mica and biotite schist illustrating the formation of the primary metamorphic foliation S1 as an axial plane cleavage to isoclinal folds F1 in the Tiang Schist formation. This foliation was subsequently affected by shear bands formed during the D2 deformation event that indicate top-to-the 190° sense of shear; (b) similar isoclinal to tight folds F1 in a larger crystallized schist containing dominantly muscovite, biotite and quartz; (c) quartzite - feldspathic meta-volcanic rock that contains large hornblende, formed during the M4 contact metamorphism event in the Tiang Schist, north of the Stong Complex contact; (d) meta-pelitic rock containing biotite, quartz feldspar and garnet, intruded in the vicinity of the sample by the Kenerong granite; (e) meta-pelitic rock intruded in the vicinity of the sample by the Kenerong granite. The rock contains large asymmetric biotite porphyroblasts indicating shearing top-to-the 120°, associated with K-feldspars in the strain shadows, quartz and sillimanite. Sillimanite crystals are aligned with the penetrative foliation and wrap around the porphyroblasts, indicating a significant flattening after mineral growth in the Kenerong granite; (f) andalusite porphyroblast within a fine grained matrix of biotite, muscovite and quartz, affected by significant flattening post-dating mineral growth in the Tiang Schist, north of the Stong Complex; (g) meta-pelitic rock from the northern part of the Stong Complex (near Jeli) showing an association of andalusite, biotite, white mica, K-feldspar, quartz and chlorite. The growth of the andalusite porphyroblast is related to the contact metamorphic event M4. The youngest phase of the deformation observed in this sample is the fracturing of the andalusite, which created the shear-bands in the phyllosilicate rich domains of the sample, where the biotite is replaced by chlorite during D4 shearing and retrograde metamorphism. C-shear band structures indicate a top-to-the 145° sense of shear.



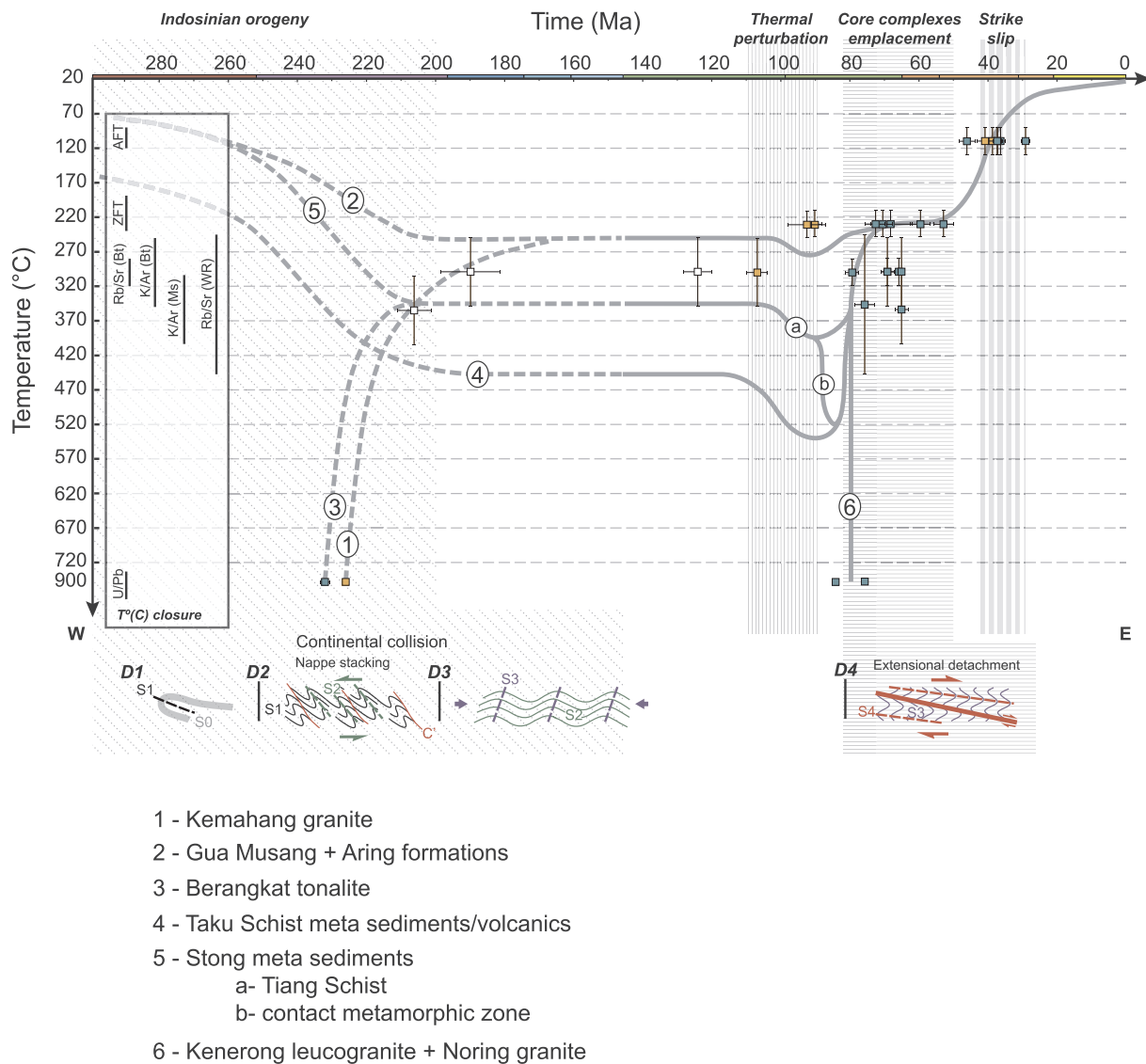


**Fig. 8.** Generalized temperature-time histories illustrating the thermal evolution of the various units in the hanging- and footwalls of the Stong Complex and Taku Schist correlated with the available thermo-chronological data. High-temperature correlation points and their error bars were compiled from existing studies (Bignell and Snelling, 1977a; Cottam et al., 2013; Darbyshire, 1988; Hughes and Bateson, 1967; Ishihara et al., 1980; Ng et al., 2015). The white colour data represent the extension of the Kemahang granite in Thailand (i.e. Buke granite) (Cobbing et al., 1992). Vertical periods are periods of rock heating or cooling. Units in the hanging wall of the Taku detachment: 1 - Kemahang granite; 2 - Gua Musang and Aring formations. Units in the footwall of the Taku detachment: 3 - Berangkat tonalite; 4 - Taku Schist meta- sediments and volcanics; 5 - Stong Complex metasediments, (a) Tiang Schist, and (b) contact metamorphic zone; 6 - Kenerong leucogranite and Noring granite. The Indosinian collision accelerated the burial of Stong, Taku, Gua Musang and Aring meta-sediments and led to the emplacement of the Kemahang and Berangkat plutons at different temperature levels. The ~100–90 Ma regional thermal perturbation (Cottam et al., 2013) re-heated all the studied units. The emplacement of the pluton increased the temperature of the Stong sediments in the contact metamorphic zone. Rapid exhumation of the Stong Complex and Taku Schist took place at different temperature levels during the Late Santonian - Early Maastrichtian activation of the Taku detachment, and was followed by further cooling related to the emplacement of the Noring pluton and subsequent erosional exhumation. Eocene - Oligocene tectonic exhumation is inferred to have taken place during a regional strike-slip event that was likely transpressional in the study area.

the Sibumasu continental unit and the Sukhothai arc (Arboit et al., 2015, 2016a; Hutchison, 2009; Metcalfe, 2013b; Sone and Metcalfe, 2008) is compatible with our observed phase of burial and shearing, demonstrated by the Permo-Triassic high-temperature absolute age dating. The Late Cretaceous intrusions are not affected by these deformations. In all areas of the Stong Complex, Taku Schist, Tiang Schist, Gua Musang and Aring formations, the D1 deformation was lead to the formation of the primary composite metamorphic foliation and associated isoclinal folding, followed by D2 top- W-SW shearing. The syn-kinematic character of the  $226.7 \pm 2.2$  Ma Kemahang granite suggests that D2 is late Middle to earliest Late Triassic. This demonstrates that the onset of burial and metamorphism that created the D1 deformation is older and may have commenced sometime during the late Palaeozoic subduction of the Paleo-Tethys Ocean or during the

latest Palaeozoic - Early Triassic collision (Fig. 8, Metcalfe, 2000). This timing would be compatible with the inference that the amphibolite-facies melange of meta- sediments and meta- mafic/acid intrusions/extrusions observed in the Taku Schist is part of a deeply buried equivalent of the Bentong-Raub suture zone (see also Md Ali et al., 2016). The D1 deformation also affected the (upper) greenschist-facies of the Tiang Schist with its (volcani-)clastic protolith, located along the eastern margin of the Western Belt and forming part of the Sibumasu continental unit. This supports evidence that D1 deformation took place also during the onset of the latest Palaeozoic - Early Triassic collision. Our microstructural observations in the Stong Complex show that a relict D1 foliation can be still recognized in meta-sedimentary rocks situated in the vicinity, yet these rocks have been affected by the Late Cretaceous magmatism and migmatization that reached (upper) am-



phibolite-facies, an effect that decreases away from these plutons. These observations show that the Latest Palaeozoic - Early Triassic burial resulted in greenschist-facies meta-sediments in the Stong Complex, while the subsequent amphibolite-facies is an effect of contact metamorphism related to the emplacement of Late Cretaceous syn-kinematic plutons. The distribution of this initial greenschist-facies metamorphism in the Stong Complex and amphibolite-facies in the Taku Schist is compatible with the geometry of the subduction/collision system, whereby the Sibumasu continental unit was differentially buried beneath the accretionary wedge and tectonically overlying Sukhotai arc. This initial nappe stack geometry implies that metamorphic rocks presently situated more eastwards were more deeply buried by thrusting and that their present surface exposure is an effect of subsequent exhumation. Obviously, this is a first order inference that may be improved by further detailed thermo-barometry studies of metamorphosed sediments.

The D2 deformation event is recorded by top- W to SW shearing and asymmetric folding, both in the higher temperature metamorphic facies of the Stong Complex, Taku Schist and Tiang Schist as well as in the lower to sub- greenschist-facies in the surrounding Gua Musang and Aring formations, where brittle thrusting with a similar E-W to NE-SW contraction direction is observed. The ductile shearing is recorded in both the Stong Complex and Taku Schist (Fig. 3). Given the available superposition criteria, this probably reflects an effect of the thrusting of the Sukhotai arc over the Sibumasu continental unit. Outside the general Late Palaeozoic - Triassic age inferred by field observations and existing thermo-chronological data, there are no further timing constraints in our study to separate D2 shearing from D1 burial. One can, however, separate D1 and D2 deformations by using existing tectono-stratigraphic constraints that show a two-stage collision (Latest Palaeozoic - Early Triassic and Middle - Late Triassic, respectively, Fig. 8, Metcalfe, 2013b). This means that D2 shearing probably took place during the emplacement of the Middle - Late Triassic plutons, which would be compatible with the local shearing observed in the Berangkat tonalite and Kemahang granite (Fig. 8). Sedimentation of the Middle Triassic Semantan Formation (Metcalfe, 2000) in a marine to continental fore-arc basin overlying the accretionary wedge implies less burial and thrusting of the continental lower plate (e.g., Fuller et al., 2006; Hansberry et al., 2015; Arboit et al., 2016b; Noda, 2016) and, therefore, also implies that D2 deformation is Late Triassic. However, it is more likely that the overall burial and thrusting was more a continuous process that took place gradually as the rocks approached the (continental) subduction zone. This means that thrusting was initiated earlier in the metamorphosed Bentong-Raub accretionary melange of the Taku Schist and later in the metamorphosed sediments of the Sibumasu sedimentary cover of the Stong Complex.

D3 contraction created open symmetrical folds and reflects the continuation of the Indosinian deformation or a subsequent episode. Our field kinematic data show that this deformation event must post-date the Middle - Early Late Triassic, because it affected the Berangkat and Kemahang plutons. Orogenic studies show that locking the subduction zone during continental collision commonly leads to continuation of contraction and the formation of more symmetric thick-skinned structures in the nappe stack or at greater distances from the orogen (e.g., Matenco et al., 2010; Ziegler et al., 1995). Following this reasoning, the symmetric shortening could reflect a continuation of earlier events during the last Early Jurassic stages of Indosinian contraction, as has been observed in neighbouring Thailand (e.g., Morley et al., 2011). However, we cannot completely exclude the possibility that the symmetric structures significantly post-date the Indosinian orogenic cycle and may actually be coeval with the regional folding observed in the Jurassic - Cretaceous red-beds (although the geometry and scale of deformation is not compatible and post-dates all other observed deformations). In this respect, the Late Cenomanian - earliest Coniacian ZFT ages obtained in the Kemahang and Eastern Belt Nal-Terekak granites may reflect either a period of tectonic exhumation

created by our D3 shortening event or the long-term erosional breakdown of an earlier created orogenic topography. Our field observations and the inferred exhumation pathway for the areas outside the Stong Complex and Taku Schist (i.e., their hanging-wall, Fig. 8) support the latter hypothesis.

## 5.2. Late Cretaceous extension associated with magmatism and exhumation

Field and microstructural observations in the Stong Complex demonstrate that D4 top-SE shearing took place initially during the emplacement of the Kenerong leucogranite and the deformed set of migmatites. In other words, D4 shearing initiated during the Late Santonian - Early Campanian (~84–75 Ma) emplacement of the Kenerong pluton. At farther distances from these magmatic rocks, the high-temperature amphibolite-facies character of the pervasive shearing associated with metasomatism decreases to greenschist-facies, which shows that the high-temperature is a localized effect near the Late Cretaceous Stong Complex plutons. Following the initial magmatic emplacement, shearing associated with retrograde metamorphism continued, with a gradual transition to more brittle cataclastic structures and normal faults indicative for compatible NW-SE extension. At greater distances from the Late Cretaceous plutons, the top-SE ductile shearing was associated with retrograde metamorphism observed by chloritisation and grain size reduction, such as observed in the Tiang Schist. All these observations demonstrate that D4 deformation took place during exhumation, the spatially-limited temperature increase during shearing in the vicinity of the plutons and migmatites being a contact metamorphism effect. The emplacement of the Noring pluton at ~75–76 Ma (Middle Campanian) took place during the last stages of tectonic exhumation as shown by its limited shearing at the brittle - ductile transition in marginal areas and by its cataclastic contact with the neighbouring Gua-Musang formation. The ZFT thermo-chronological ages from the Kenerong leucogranite and Berangkat tonalite at farther distances from the Noring pluton (PM13 and P20, Fig. 3a) reflect this gradual tectonic exhumation, during which temperatures decreased to ~220 °C at ~74–69 Ma (Late Campanian - Early Maastrichtian). In these samples, the tectonic exhumation was high enough to reset the ZFT samples, but beneath the AFT closure temperature, which shows Eocene-Oligocene ages (Fig. 3). Therefore, the Late Santonian - Early Maastrichtian deformation exhumed the Stong Complex to temperatures between 220 and 140 °C (Fig. 8). This means uplift between 8 and 5 km at a normal geothermal gradient, although this uplift was certainly higher given the regional Late Cretaceous thermal effect (Cottam et al., 2013), as indicated by the geobarometry of the Noring pluton (Ghani, 2000c). The three ZFT ages of ~74–53 Ma obtained in the Noring granite and its vicinity (P14, P19 and P22, Fig. 3a) cannot be discriminated in terms of magmatic cooling versus tectonic exhumation: the older age is very close to the age of pluton, while the younger age may also reflect longer term magmatic cooling or subsequent erosional breakdown following the main Late Santonian - Early Maastrichtian deformation (Fig. 8).

The situation is different in the metamorphosed clastic and magmatic melange of the Taku Schist. The absence of Late Cretaceous magmatism resulted in top-SE shearing associated with retrograde metamorphism to greenschist-facies accompanied by semi-brittle deformation, altogether a result of tectonic exhumation from amphibolite-facies conditions (Fig. 8). Outside the Stong Complex and Taku Schist, the Gua Musang and Aring formations do not show any significant change of their metamorphic facies in the vicinity of the Kenerong - Noring plutons, being always separated by cataclastic and brittle shear zones. Therefore, after initial burial in the sub- greenschist to lower greenschist-facies, their thermal evolution does not indicate accelerated Cretaceous exhumation (Fig. 8). Our field observations indicate that these meta-sediments unconformably overlie the Nal-Terekak granite. A Late Cenomanian - earliest Coniacian ZFT age of  $92.5 \pm 5.1$  Ma was obtained from sample P23 and, although this is still a Late Cretaceous

age, it significantly pre-dates the onset of Stong Complex tectonic exhumation and follows the same pattern of exhumation inferred for the overlying Gua Musang/Aring sediments.

All these combined observations and thermo-chronological data demonstrate that the tectonic exhumation of the Stong Complex and Taku Schist took place in response to Late Santonian - Early Maastrichtian extensional detachments that indicate a top-SE direction of shearing. The similarity of the shearing direction combined with the same mylonitisation and retrograde metamorphism effects away from the influence of Late Cretaceous plutons implies a similar genetic evolution. Therefore, we interpret that the Taku extensional detachment is responsible for the late Santonian - Early Maastrichtian tectonic exhumation in both the Stong Complex and Taku Schist. The deformation is expressed by a large array of ductile to brittle structures, formed during the gradual transition through various temperature and depth levels, perhaps also related to magmatic thermal effects. This deformation resulted in mylonites in amphibolite- to greenschist-facies meta-sediments, in syn-kinematic plutons in the footwall of the detachment, and cataclastic shearing and normal faulting in its hanging wall, cross-cutting the mylonites during the late stage footwall exhumation. Deformation was associated with folds with horizontal axial planes due to vertical flattening of inherited steep foliations. The largest detachment offset is recorded in the SE part of the Taku Schist, where a tectonic omission in the order of 300 °C is recorded (Fig. 8), which means 12–15 km of differential vertical footwall exhumation at a normal geothermal gradient (Fig. 8, Md Ali et al., 2016). The amount of mylonitisation and shearing generally decreases in a NW-ward direction in both the Stong Complex and Taku Schists, from wide mylonite and shear zones to more localized and discrete shearing associated with brittle deformation. This reflects a typical asymmetry in the footwall of such extensional detachments, with maximum exhumation and deformation in the direction of shearing, gradually decreasing in the opposite direction.

In the area connecting the Stong Complex and Taku Schist, the P8 sample of the Kemahang granite resulted in a Turonian ZFT age of  $90.3 \pm 2.2$  Ma. This predates the late Santonian onset of exhumation against the extensional detachment. Therefore, we interpret the Kemahang granite to be part of the hanging-wall structural unit of the extensional detachment (Figs. 3 and 8), an interpretation that differs from our previous conclusions (Md Ali et al., 2016). The ~107 K-Ar biotite age previously derived from the Kemahang granite (Bignell and Snelling, 1977a) cannot reflect erosional break-down exhumation and was likely influenced by a Cretaceous thermal reset in the vicinity of the extensional detachment, as discussed below.

### 5.3. Eocene-Oligocene exhumation

Our low-temperature AFT data indicate Eocene - Oligocene cooling in all samples in both the foot- and hanging- wall of the Taku detachment. In the absence of known thermal effects, such a distribution must reflect regional exhumation at the scale of our entire study area. Similar Paleogene ages have been obtained in other U-Th-Sm/He studies (Cottam et al., 2013). Although not part of our kinematic study, our field observations indicate that the large wavelength folding of the Jurassic - Cretaceous red-beds postdates all other quantified deformation. The character of this deformation is always brittle and was interpreted to be associated with significant strike-slip deformation (Mustaffa Kamal Shuib, 2000a,c, 2009a,b; Tjia, 1996, 1998). Similar Eocene - Oligocene strike-slip deformation associated with local basin formation or transpressional zones has been quantified in onshore and offshore Thailand (e.g., Morley, 2001, 2004, 2012, 2013; Morley et al., 2011; Ridd, 2012 and references therein). Interesting is the Eocene - Oligocene formation of the neighbouring Malay Basin, which was associated with transtensional tectonics along a strike-slip system that changed its geometry with time (Mansor et al., 2014). This means the formation of the Malay basin was associated with significant exhumation

in the neighbouring Peninsular Malaysia onshore region. Therefore, when combined with all these previous observations, the Eocene - Oligocene exhumation observed in our AFT ages is likely to be the result of regional strike-slip tectonics that affected the E to NE margin of the South China Sea, commonly associated with India - Asia collision (see discussion in Morley, 2013).

## 6. Towards understanding a metamorphic core-complex in the northern Peninsular Malaysia

Metamorphic core complexes form by the isostatic exhumation of lower to middle crustal rocks along extensional detachments associated with high-temperature effects (Lister and Davis, 1989; Wernicke, 1992; Wernicke and Axen, 1988). The continuity of Moho and the rather normal crustal thickness often observed during the evolution of such structures result from the rheological weakness of the lower crust, which allows lateral flow at high (~800 °C) Moho temperatures to accommodate the stretching of the upper brittle crust (Brun and Sokoutis, 2007; Buck, 1991; Ranalli et al., 1989; Sonder and England, 1989; Tirel et al., 2004). However, the continuation of extension may ultimately result in significant crustal thinning. A hot and weak high temperature lithosphere at the base of the crust may result from various geodynamic settings, such as asthenospheric plumes, long-term evolution of thickened crust, back-arc extension, delamination, slab detachment, relamination or eduction (Burov and Gerya, 2014; DeCelles et al., 2009; Ducea and Barton, 2007; Duretz and Gerya, 2013). The evolution of detachment faults and their bearing on deformation geometries is diverse, ranging from tilted blocks, rotated normal faults and simple-shear zones to the formation of extensional gneiss domes (Buck, 1988; Coletta and Angelier, 1982; Lister et al., 1991; Spencer, 1984; Tirel et al., 2004; Wernicke, 1985).

Previous studies have convincingly demonstrated that a period of significant thermal perturbation across the Peninsular Malaysia occurred at ~105–87 Ma, observed by increased temperatures in the crust, partial resetting of the Ar-Ar thermo-chronometer in widely distributed samples and an association with intrusion of basaltic dykes (Cottam et al., 2013; Ghani, 2009). Although the geodynamic reasons for such regional crustal heating are unclear, our observations demonstrate that a hot and, therefore, rheologically weak crust existed at the onset of the Late Santonian - Early Maastrichtian Stong Complex - Taku Schist extension at ~85–84 Ma. In such conditions, the initiation of the Taku extensional detachment, with its dozens of kilometres offset, resulted in the creation of significant volumes of crustal melt and widespread migmatization in its footwall, which were pervasively sheared during exhumation. Such emplacement and shearing is observed in many Mediterranean core-complexes (Brun and Faccenna, 2008; Brun and Sokoutis, 2007; Jolivet and Brun, 2010; Jolivet et al., 2013; Tirel et al., 2004). We thus suggest that the Stong Complex represents an extensional gneiss dome characterized by crustal melting and pervasive migmatization, which is partly in agreement with its highly K and per-aluminous geochemistry (Ghani, 2009; Jamin and Umor, 2001; Umor et al., 2006). Such melts are gradually generated and sheared in the vicinity of detachments, in agreement with the geometry and timing of the Kenerong and Noring granites, and implies that the pluton emplacement and migmatization were genetically related. The spatial offset between the Stong gneiss dome and the location of maximum exhumation in the meta-sediments of the Taku Schists infers that the core-complex is not a simple gneiss dome. Good analogues are the Aegean-types of core complex, where such gneiss domes are associated with rotated normal faults and simple shear, the maximum exhumation of core-complexes being observed in meta-sediments, such as for instance in the Kerdylon detachment that controls the Eocene exhumation of the southern Rhodope core-complex (Brun and Sokoutis, 2007; Jolivet and Brun, 2010). This explains also the spatial separation by the intervening Gua Musang - Aring formations of the Taku Schist and Stong Complex (Fig. 3). In such detach-

ments or core-complexes, the formation of extensional basins is fairly limited, being associated with thin sedimentation in continental conditions enhanced by the uplift induced during the initial thermal anomaly, and often spatially offset from the location of lower crustal exhumation (Balázs et al., 2016; Wernicke, 1992). The genesis of such sediments could be easily hidden in the geometry of the poorly dated Jurassic-Cretaceous redbeds, particularly in the light of their subsequent Eocene-Oligocene deformation, or in the continental sedimentation that forms the base of adjacent sedimentary basins of the South China Sea (Morley, 2012). Numerical modelling studies have shown that the presence of a suture zone favours its reactivation in large extensional detachments associated with numerous widely distributed basins filled with thin syn-rift sedimentation (Balázs et al., 2017). This geometry explains the observed reactivation of the Bentong-Raub Suture and thin continental sedimentation. The presently observed thinned crust beneath the Central Belt of Peninsular Malaysia (Ryall, 1982) cannot reflect a gradual Indosinian thickening of the crust and must have been established during the Cretaceous thermal anomaly and/or the continuation of Late Cretaceous extension along Taku-type of detachments. Obviously, all these considerations are partly speculative with the data available to the present study; a further understanding of the geochemistry of the plutons, the migmatization process, regional kinematic analysis and the genetic link with the widespread continental sedimentation is required.

## 7. Conclusions

This combined kinematic and thermo-chronological study in the northeastern part of Peninsular Malaysia has demonstrated a novel tectonic interpretation that builds upon the availability of previous tectono-stratigraphic and thermochronological constraints. Our study shows that the Indosinian orogenic evolution is reflected in the structure of the Stong Complex and Taku Schist in successive burial, shearing and other episodes of contraction. These events brought the Sibumasu sedimentary cover together with the accretionary wedge and genetically associated Bentong-Raub melange to various greenschist- to amphibolite- facies conditions depths, controlled by their position relative to the Sukhotai arc upper plate. The widespread shearing indicates top- W to SW directions of tectonic transport that in places are surprisingly oblique to the present N-S general trend of the orogenic structure.

This orogenic structure was subsequently influenced by a Cretaceous thermal anomaly that culminated with the formation of the Late Santonian - Early Maastrichtian Taku extensional detachment, which shows top-SE directions of tectonic transport. The detachment evolution was genetically related to the generation of decompression melts in the crust and the emplacement of the Kenerong and Noring granites and to the associated crustal migmatization observed in the Stong Complex. The magmatic and sedimentary rocks of the Bentong-Raub suture and the Sibumasu cover previously metamorphosed to greenschist-facies conditions in the Stong Complex were affected by shearing and pro-grade contact metamorphism to amphibolite-facies conditions in the vicinity of the plutons, and later by continued shearing and retro-grade metamorphism during the gradual exhumation in the footwall of the detachment. The Bentong-Raub and accretionary melange previously metamorphosed to amphibolite-facies conditions in the Taku Schist was affected by direct shearing and retro-grade metamorphism in the footwall of the detachment and the creation of a 15–20 km tectonic crustal omission. This dual thermal evolution has created a wide array of structures formed during the activity of the Taku detachments, varying from thick zones of amphibolite-facies mylonites to more focussed greenschist-facies shearing and ultimately to cataclastic zones of deformation and normal faulting accompanied by folds with sub-horizontal axial planes caused by flattening of steep foliation.

This evolution was followed by renewed Eocene - Oligocene

exhumation observed in our apatite fission track data. Correlation with previous local or more regional studies implies that this phase of tectonic exhumation formed in response to strike-slip tectonic accommodation zones of uplift or other areas of sedimentary basin formation, as observed elsewhere in the NW part of the South China Sea and its adjacent onshore areas.

Although more research is needed to quantify the Late Cretaceous extension in Peninsular Malaysia, we suggest that an initial Cretaceous thermal anomaly played a fundamental role in the development of an extensional gneiss dome associated with simple shear and normal fault rotation that was controlled by the Taku detachment. The formation of genetically related extensional basins could have shifted elsewhere, while continental environments could have been favoured by the thermal anomaly driven uplift.

## Acknowledgements

This study is the result of the joint collaboration between the Netherlands Centre for Integrated Solid Earth Science, University of Utrecht, The Netherlands and the University of Malaya, Kuala Lumpur, Malaysia (Grant no. RU011-2013). H. Doust is acknowledged for a detailed revision of the manuscript and for his opening of the collaboration between Utrecht University and University of Malaya. The anonymous reviewers are gratefully acknowledged for their constructive comments that have improved the quality of the manuscript.

## References

- Abdullah, Ibrahim, Setiawan, Jatmika, 2003. The kinematics of deformation of the Kenerong Leucogranite and its enclaves at Renyok waterfall, Jeli, Kelantan. *Bull. Geol. Soc. Malaysia* 46, 307–312.
- Alexander, J.B., 1959. Pre-tertiary stratigraphic succession in Malaya. *Nature* 183, 230–231.
- Aragon-Arreola, M., Martin-Barajas, A., 2007. Westward migration of extension in the northern Gulf of California, Mexico. *Geology* 35, 571–574.
- Arboit, F., Amrouch, K., Collins, A.S., King, R., Morley, C., 2015. Determination of the tectonic evolution from fractures, faults, and calcite twins on the southwestern margin of the Indochina Block. *Tectonics* 34, 1576–1599.
- Arboit, F., Collins, A.S., Morley, C.K., King, R., Amrouch, K., 2016a. Detrital zircon analysis of the southwest Indochina terrane, central Thailand: unravelling the Indosinian orogeny. *Geol. Soc. Am. Bull.* 128, 1024–1043.
- Arboit, F., Collins, A.S., Morley, C., King, R., Amrouch, K., 2016b. Geochronological and geochemical study of mafic dykes from the Khao Khwang Fold-Thrust Belt: implications for petrogenesis and tectonic evolution. *Gondwana Res.* 36, 124–141.
- Aw, P.C., 1974. Geology of the Sungai Nenggiri - Sunggai betis area. Geological Survey of Malaysia Annual Report, 1972 sheet 44, pp. 115–119.
- Aw, P.C., 1990. Geology and mineral resources of the Sungai Aring area, Kelantan Darul Naim. *Geol. Surv. Malaysia District Memoir* 21, 116.
- Bacho, Ramdanhshah, Umor, M.R., 2001. Geokimia Tonalit Berangkat dan Leukogranit Kenerong sebagai petunjuk kepada pembentukan dan asalan magma Kompleks Stong, Kelantan. Proceedings, Geological Society of Malaysia Annual Conference 2001, 147–154.
- Baïoumy, H., Ulfa, Y., 2016. Facies analysis of the Semanggol Formation, South Kedah, Malaysia: a possible Permian-Triassic boundary section. *Arab. J. Geosci.* 9, 1–16.
- Balázs, A., Matenco, L., Magyar, I., Horváth, F., Cloetingh, S., 2016. The link between tectonics and sedimentation in back-arc basins: new genetic constraints from the analysis of the Pannonian Basin. *Tectonics* 35, 1526–1559.
- Balázs, A., Burov, E., Matenco, L., Vogt, K., François, T., Cloetingh, S., 2017. Symmetry during the syn- and post-rift evolution of extensional back-arc basins: the role of inherited orogenic structures. *Earth Planet. Sci. Lett.* 462, 86–98.
- Barbarand, J., Hurford, T., Carter, A., 2003. Variation in apatite fission-track length measurement: implications for thermal history modelling. *Chem. Geol.* 198, 77–106.
- Bernet, M., Spiegel, C., 2004. Detrital Thermochronology - Provenance Analysis, Exhumation, and Landscape Evolution of Mountain Belts. The Geological Society of America.
- Bignell, J.D., Snelling, N.J., 1977a. Geochronology of Malayan Granites. Institute of Environmental Sciences, Natural Environment Research Council, London, pp. 70.
- Bignell, J.D., Snelling, N.J., 1977b. K-Ar ages on some basic igneous rocks from Peninsular Malaysia and Thailand. *Bull. Geol. Soc. Malaysia* 8, 89–93.
- Brandon, M.T., 1992. Decomposition of fission-track grain-age distributions. *Am. J. Sci.* 292, 535–564.
- Brun, J.-P., Faccenna, C., 2008. Exhumation of high-pressure rocks driven by slab rollback. *Earth Planet. Sci. Lett.* 272, 1–7.
- Brun, J.-P., Sokoutis, D., 2007. Kinematics of the southern Rhodope core complex (North Greece). *Int. J. Earth Sci.* 96, 1079–1099.
- Buck, W.R., 1988. Flexural rotation of normal faults. *Tectonics* 7, 959–973.
- Buck, W.R., 1991. Modes of continental lithospheric extension. *J. Geophys. Res.* 96,



- 20161–20178.
- Burov, E., Gerya, T., 2014. Asymmetric three-dimensional topography over mantle plumes. *Nature* 513, 85–89.
- Burtner, R.L., Nigrini, A., Donelick, R.A., 1994. Thermochronology of lower cretaceous source rocks in the idaho-wyoming thrust belt. *AAPG Bull.* 78, 1613–1636.
- Cobbing, E.J., Pitfield, P.E.J., Darbyshire, D.B.F., Mallik, D.I.J., 1992. The Granites of the South East Asian Tin Belt. British Geological Survey, London.
- Coletta, B., Angelier, J., 1982. Sur les systemes de blocs failles basculées associées aux fortes extensions: etude preliminaire d'exemples ouestamericains (Nevada, USA et Basse California, Mexique). *Academie de Sciences Compte Rendus* 294, 467–469.
- Cottam, M.A., Hall, R., Ghani, A.A., 2013. Late cretaceous and cenozoic tectonics of the Malay Peninsula constrained by thermochronology. *J. Asian Earth Sci.* 76, 241–257.
- Cox, S.F., Paterson, M.S., 1991. Experimental dissolution-precipitation creep in quartz aggregates at high temperatures. *Geophys. Res. Lett.* 18, 1401–1404.
- Darbyshire, D.B.F., 1988. Geochronology of Malaysian Granites. Natural Environment Research Council, Isotope Geology Report, British Geological Survey.
- DeCelles, P.G., Ducea, M.N., Kapp, P., Zandt, G., 2009. Cyclicity in Cordilleran orogenic systems. *Nat. Geosci.* 2, 251–257.
- Dewey, J.F., 1988. Extensional collapse of orogens. *Tectonics* 7, 1123–1139.
- Doglion, C., Carminati, E., Cuffaro, M., Scrocca, D., 2007. Subduction kinematics and dynamic constraints. *Earth Sci. Rev.* 83, 125–175.
- Ducea, M.N., Barton, M.D., 2007. Igniting flare-up events in Cordilleran arcs. *Geology* 35, 1047–1050.
- Duretz, T., Gerya, T.V., 2013. Slab detachment during continental collision: influence of crustal rheology and interaction with lithospheric delamination. *Tectonophysics* 602, 124–140.
- Faccenna, C., Becker, T.W., Auer, L., Billi, A., Boschi, L., Brun, J.P., Capitanio, F.A., Funiello, F., Horvath, F., Jolivet, L., Piromallo, C., Royden, L., Rossetti, F., Serpelloni, E., 2014. Mantle dynamics in the Mediterranean. *Rev. Geophys.* 52, 283–332.
- Foeken, J.P.T., 2004. Tectono-morphology of the Ligurian Alps and adjacent basins (NW Italy): an integrated study of their neogene to present evolution. PhD Thesis, VU University Amsterdam, The Netherlands, pp. 192.
- Foo, K.Y., 1983. The Palaeozoic sedimentary rocks of Peninsular Malaysia – stratigraphy and correlation. In: *Proceedings of the Workshop on Stratigraphic Correlation of Thailand and Malaysia*, 1: Technical Papers. Geological Society of Thailand & Geological Society of Malaysia, pp. 1–19.
- Froitzheim, N., Conti, P., van Daalen, M., 1997. Late Cretaceous, synorogenic, low-angle normal faulting along the Schilling fault (Switzerland, Italy, Austria) and its significance for the tectonics of the Eastern Alps. *Tectonophysics* 280, 267–293.
- Fuller, C.W., Willett, S.D., Brandon, M.T., 2006. Formation of forearc basins and their influence on subduction zone earthquakes. *Geology* 34, 65–68.
- Galbraith, R.F., 1981. On statistical models for fission track counts. *Math. Geol.* 13, 471–478.
- Galbraith, R.F., Laslett, G.M., 1993. Statistical-models for mixed fission-track ages. *Nucl. Tracks Rad. Meas.* 21, 459–470.
- Gallagher, K., 2012. Transdimensional inverse thermal history modeling for quantitative thermochronology. *J. Geophys. Res.: Solid Earth* 117 n/a–n/a.
- Gallagher, K., Charvin, K., Nielsen, S., Sambridge, M., Stephenson, J., 2009. Markov chain Monte Carlo (MCMC) sampling methods to determine optimal models, model resolution and model choice for Earth Science problems. *Mar. Pet. Geol.* 26, 525–535.
- Garver, J.I., 2003. Etching zircon age standards for fission-track analysis. *Radiat. Meas.* 37, 47–53.
- Ghani, A.A., 2000a. Hornblende chemistry and its application to geobarometry of the norning pluton, stong complex, Kelantan. *Proceedings, Geological Society of Malaysia Annual Conference 2000*, 81–86.
- Ghani, A.A., 2000b. Mantled feldspar from the Noring granite, Peninsular Malaysia: petrography, chemistry and petrogenesis. *Bull. Geol. Soc. Malaysia* 44, 109–115.
- Ghani, A.A., 2000c. The Western Belt granite of Peninsular Malaysia: some emergent problems on granite classification and its implication. *Geosci. J.* 4, 283–293.
- Ghani, A.A., 2009. Plutonism. In: Hutchison, C.S., Tan, D.N.K. (Eds.), *Geology of Peninsular Malaysia*. University of Malaya and Geological Society of Malaysia, Kuala Lumpur, Malaysia, pp. 211–232.
- Gleadow, A.J.W., Duddy, I.R., 1981. A natural long-term track annealing experiment for apatite. *Nucl. Tracks* 5, 169–174.
- Green, P.F., 1985. Comparison of zeta calibration baselines for fission-track dating of apatite, zircon and sphene. *Chem. Geol.: Isotope Geosci. Sect.* 58, 1–22.
- Hall, R., 2011. Australia–SE Asia collision: plate tectonics and crustal flow. *Geol. Soc., London, Spec. Publ.* 355, 75–109.
- Hall, R., 2012. Late Jurassic–Cenozoic reconstructions of the Indonesian region and the Indian Ocean. *Tectonophysics* 570–571, 1–41.
- Hansberry, R.L., Collins, A.S., King, R., Morley, C., Gize, A.P., Warren, J., Löhr, S.C., Hall, P.A., 2015. Syn-deformation temperature and fossil fluid pathways along an exhumed detachment, Khao Khwang Fold-Thrust Belt, Thailand. *Tectonophysics* 655, 73–87.
- Harbury, N.A., Jones, M.E., Audley-Charles, M.G., Metcalfe, I., Mohamed, K.R., 1990. Structural evolution of mesozoic Peninsular Malaysia. *J. Geol. Soc.* 147, 11–26.
- Harun, Z., 2002. Late mesozoic-early tertiary faults of Peninsular Malaysia. *Bull. Geol. Soc. Malaysia* 45, 117–120.
- Harun, Z., Jasin, B., Mohsin, N., Azami, A., 2009. Thrust in the Semanggol formation, Kuala Ketil, Kedah. *Bull. Geol. Soc. Malaysia* 55, 61–66.
- Hughes, I.G., Bateson, J.H., 1967. Reconnaissance geological and mineral survey of the Chanthaburi area of South-east Thailand. Institute of Geological Sciences.
- Hurford, A.J., Green, P.F., 1982. A users' guide to fission track dating calibration. *Earth Planet. Sci. Lett.* 59, 343–354.
- Hutchison, C.S., 1969. Some notes on the Stong metamorphic complex, Kelantan. *Geol. Soc. Malaysia Newsletter* 21, 8–11.
- Hutchison, C.S., 1973a. Metamorphism. In: Gobbett, D.J., Hutchison, C.S. (Eds.), *Geology of the Malay Peninsula*. Wiley - Interscience, New York, pp. 253–303.
- Hutchison, C.S., 1973b. Plutonic activity. In: Gobbett, D.J., Hutchison, C.S. (Eds.), *Geology of the Malay Peninsula*. Wiley - Interscience, New York, pp. 215–252.
- Hutchison, C.S., 1973c. Tectonic evolution of Sundaland: a phanerozoic synthesis. *Bull. Geol. Soc. Malaysia* 6, 61–86.
- Hutchison, C.S., 1975. Ophiolite in Southeast Asia. *Geol. Soc. Am. Bull.* 86, 797–806.
- Hutchison, C.S., 1977. Granite emplacement and tectonic subdivision of Peninsular Malaysia. *Bull. Geol. Soc. Malaysia* 9, 187–207.
- Hutchison, C.S., 1989. Geological Evolution of South-East Asia. Clarendon Press, Oxford.
- Hutchison, C.S., 1994. Gondwana and Cathaysian blocks, palaeotethys sutures and cenozoic tectonics in South-east Asia. *Geol. Rundsch.* 83, 388–405.
- Hutchison, C.S., 2009. Metamorphism. In: Hutchison, C.S., Tan, D.N.K. (Eds.), *Geology of Peninsular Malaysia*. University of Malaya and Geological Society of Malaysia, Kuala Lumpur, Malaysia, pp. 233–247.
- Hutchison, C.S., 2014. Tectonic evolution of Southeast Asia. *Bull. Geol. Soc. Malaysia* 60, 1–18.
- Hutchison, C.S., Tan, D.N.K., 2009. *Geology of Peninsular Malaysia*. University of Malaya and Geological Society of Malaysia, Kuala Lumpur, Malaysia.
- Hyndman, R.D., Currie, C.A., Mazzotti, S.P., 2005. Subduction zone backarcs, mobile belts, and orogenic heat. *GSA Today* 15, 4–10.
- Ishihara, S., Sawata, H., Shibata, K., Terashima, S., Arriyul, S., Sato, K., 1980. Granites and Sn-W deposits of peninsular Thailand. *Mining Geol. Spec. Issue* 8, 223–241.
- Ismail, H.H., Madon, M., Bakar, Z.A.A., 2007. Sedimentology of the Semantan Formation (Middle - Upper Triassic) along the Karak-Kuantan Highway, central Pahang. *Bull. Geol. Soc. Malaysia* 53, 27–34.
- Jamin, N.H.M., Umor, M.R., 2001. Komplek Stong: Kajian geokimia ke atas batuan Granit Noring dan Leukogranit Kenerong di Kampung Renyok, Jeli, Kelantan. *Proceedings, Geological Society of Malaysia Annual Conference 2001*, 161–167.
- Jasin, B., 2013. Chert blocks in Bentong-Raub Suture Zone: A heritage of palaeo-tethys. *Bull. Geol. Soc. Malaysia* 59, 85–91.
- Jasin, B., Harun, Z., 2007. Stratigraphy and sedimentology of the chert unit of the semanggol formation. *Bull. Geol. Soc. Malaysia* 53, 103–109.
- Jolivet, L., Brun, J.-P., 2010. Cenozoic geodynamic evolution of the Aegean. *Int. J. Earth Sci.* 99, 109–138.
- Jolivet, L., Faccenna, C., Huet, B., Labrousse, L., Le Pourhiet, L., Lacombe, O., Lecomte, E., Burov, E., Denèle, Y., Brun, J.-P., Philippon, M., Paul, A., Salain, G., Karabulut, H., Piromallo, C., Monié, P., Gueydan, F., Okay, A.I., Oberhänsli, R., Poureteau, A., Augier, R., Gadenne, L., Driussi, O., 2013. Aegean tectonics: strain localisation, slab tearing and trench retreat. *Tectonophysics* 597–598, 1–33.
- Khoo, T.T., 1980. Some comments on the emplacement level of the Kemahang granite, Kelantan. *Bull. Geol. Soc. Malaysia* 13, 93–101.
- Khoo, T.T., 1983. Metamorphic episodes of the western foothills of Gunung Ledang (Mt. Ophir), Johore-Malacca, with a background account on the geology. *Bull. Geol. Soc. Malaysia* 16, 117–138.
- Khoo, K.K., 1998. *Geology and Mineral Resources of the Kuala Pilah Area, Negeri Sembilan*. Geological Survey of Malaysia Map Report 11, 93 pp.
- Khoo, T.T., Lim, S.P., 1983. Nature of the contact between the Taku Schists and adjacent rocks in the Manek Urai area, Kelantan and its implications. *Bull. Geol. Soc. Malaysia* 16, 139–158.
- Konjing, Z., Malihan, M., Said, U., 2007. Jurassic-Cretaceous continental deposits from Eastern Chenor, Pahang. *Bull. Geol. Soc. Malaysia* 53, 7–10.
- Krahenbuhl, R., 1991. Magmatism, tin mineralisation and tectonics of the main range, Malaysian Peninsula: consequences for the plate tectonic model of the Southeast Asia based on Rb-Sr, K-Ar and fission track data. *Bull. Geol. Soc. Malaysia* 29, 1–100.
- Kwan, T.S., 1990. K-Ar dating of micas from granitoids in the Kuala Lumpur - Seremban area. *Bull. Geol. Soc. Malaysia* 26, 77–96.
- Lee, C.P., 2009. Palaeozoic stratigraphy. In: Hutchison, C.S., Tan, D.N.K. (Eds.), *Geology of Peninsular Malaysia*. University of Malaya and Geological Society of Malaysia, Kuala Lumpur, Malaysia, pp. 55–86.
- Lee, C.P., Mohd, S.L., Kamaludin, H., Bahari, M.N., Rashidah, K., 2014. *Stratigraphic Lexicon of Malaysia*. Geological Society of Malaysia, Kuala Lumpur.
- Lister, G.S., Davis, G.A., 1989. The origin of metamorphic core complexes and detachment faults formed during tertiary continental extension in the Northern Colorado River Region, USA. *J. Struct. Geol.* 11, 65–94.
- Lister, G.A., Etheridge, M.A., Symonds, P.A., 1991. Detachment models for the formation of passive continental margins. *Tectonics* 10, 1038–1064.
- MacDonald, S., 1968. The geology and mineral resources of north Kelantan and north Terengganu. *Geol. Survey Dept. West Malaysia Memoir* 10, 202.
- MacDonald, A.S., Barr, S.M., Dunning, G.R., Yaowanoyothin, W., 1993. The Doi Inthanon metamorphic core complex in NW Thailand: age and tectonic significance. *J. SE Asian Earth Sci.* 8, 117–125.
- Madon, M., 2010. Submarine mass-transport deposits in the Semantan formation (middle-upper Triassic), central Peninsular Malaysia. *Bull. Geol. Soc. Malaysia* 56, 15–26.
- Madon, M., Bakar, Z.A.A., Ismail, H.H., 2010. Jurassic-Cretaceous fluvial channel and floodplain deposits along the Karak-Kuantan Highway, central Pahang (Peninsular Malaysia). *Bull. Geol. Soc. Malaysia* 56, 9–14.
- Mansor, M.Y., Rahman, A.H.A., Menier, D., Pubellier, M., 2014. Structural evolution of Malay Basin, its link to Sunda Block tectonics. *Mar. Pet. Geol.* 58 (Part B), 736–748.
- Matenco, L., Krézsek, C., Merten, S., Schmid, S., Cloetingh, S., Andriessen, P., 2010. Characteristics of collisional orogens with low topographic build-up: an example from the Carpathians. *Terra Nova* 22, 155–165.
- Md Ali, M.A., Willingshofer, E., Matenco, L., Francois, T., Daanen, T.P., Ng, T.F., Taib, N.I., Shuib, M.K., 2016. Kinematics of post-orogenic extension and exhumation of the Taku Schist, NE Peninsular Malaysia. *J. Asian Earth Sci.* 127, 63–75.
- Metcalfe, I., 2000. The Bentong-Raub suture zone. *J. Asian Earth Sci.* 18, 691–712.

- Metcalfe, I., 2011. Tectonic framework and phanerozoic evolution of Sundaland. *Gondwana Res.* 19, 3–21.
- Metcalfe, I., 2013a. Gondwana dispersion and Asian accretion: tectonic and palaeogeographic evolution of eastern Tethys. *J. Asian Earth Sci.* 66, 1–33.
- Metcalfe, I., 2013b. Tectonic evolution of the Malay Peninsula. *J. Asian Earth Sci.* 76, 195–213.
- MGD (Minerals and Geoscience Department Malaysia), 2013. Geological Map of the Kampung Batu Melintang Area, Peninsular Malaysia. Scale 1:63,360, Minerals and Geoscience Department Malaysia, Kuala Lumpur, Malaysia.
- Mohd Shafeea Leman, 2004. Part 2: Mesozoic. In: Lee, C.P., Mohd Shafeea Leman, Hassan, K., Md. Nasib, B., Karim, R. (Eds.), *Stratigraphic Lexicon of Malaysia*. Geological Society of Malaysia, p. 176.
- Morley, C.K., 2001. Combined escape tectonics and subduction rollback-back arc extension: a model for the evolution of Tertiary rift basins in Thailand, Malaysia and Laos. *J. Geol. Soc.* 158, 461–474.
- Morley, C.K., 2004. Nested strike-slip duplexes, and other evidence for late cretaceous-paleogene transpressional tectonics before and during India-Eurasia collision, in Thailand, Myanmar and Malaysia. *J. Geol. Soc.* 161, 799–812.
- Morley, C.K., 2012. Late cretaceous - early paleogene tectonic development of SE Asia. *Earth Sci. Rev.* 115, 37–75.
- Morley, C.K., 2013. Discussion of tectonic models for Cenozoic strike-slip fault-affected continental margins of mainland SE Asia. *J. Asian Earth Sci.* 76, 137–151.
- Morley, C.K., Charusiri, P., Watkinson, I.M., 2011. Structural geology of Thailand during the Cenozoic. In: Ridd, M.F., Barber, A.J., Crow, M.J. (Eds.), *The Geology of Thailand*. Geological Society of London, London, pp. 273–334.
- Mustaffa Kamal Shuib, 2000a. The mesozoic tectonics of peninsular Malaysia – an overview. In: *GSM Dynamic Stratigraphy & Tectonics of Peninsular Malaysia – Seminar III. The Mesozoic of Peninsular Malaysia*. Geological Society of Malaysia Warta Geologi, pp. 23–29 26.
- Mustaffa Kamal Shuib, 2000b. The olistostromes in the Bentong area, Pahang and their tectonic implications. *Proceedings, Geological Society of Malaysia Annual Conference 2000*, 51–55.
- Mustaffa Kamal Shuib, 2000c. Syndepositional deformations in the Permo-triassic and latest triassic to cretaceous central basins of Peninsular Malaysia. In: *Dynamic Stratigraphy & Tectonics of Peninsular Malaysia – Seminar III. The Mesozoic of Peninsular Malaysia*. Geological Society of Malaysia, pp. 30–47 26.
- Mustaffa Kamal Shuib, 2009a. Major faults. In: Hutchison, C.S., Tan, B.K. (Eds.), *Geology of Peninsular Malaysia*. University of Malaya, Kuala Lumpur, pp. 249–269.
- Mustaffa Kamal Shuib, 2009b. Structures and deformation. In: Hutchison, C.S., Tan, B.K. (Eds.), *Geology of Peninsular Malaysia*. University of Malaya, Kuala Lumpur, pp. 271–308.
- Ng, T.F., 1994. Microstructures of the deformed granites of eastern Kuala Lumpur - implications for mechanisms and temperatures of deformation. *Bull. Geol. Soc. Malaysia* 35, 47–59.
- Ng, S.W.-P., Whitehouse, M.J., Searle, M.P., Robb, L.J., Ghani, A.A., Chung, S.-L., Oliver, G.J.H., Sone, M., Gardiner, N.J., Roselee, M.H., 2015. Petrogenesis of Malaysian granitoids in the Southeast Asian tin belt: Part 2. U-Pb zircon geochronology and tectonic model. *Geol. Soc. Am. Bull.*
- Noda, A., 2016. Forearc basins: types, geometries, and relationships to subduction zone dynamics. *Geol. Soc. Am. Bull.* 128, 879–895.
- Nuraiteng Tee Abdullah, 2009. Mesozoic stratigraphy. In: Hutchison, C.S., Tan, D.N.K. (Eds.), *Geology of Peninsular Malaysia*. University of Malaya and Geological Society of Malaysia, Kuala Lumpur, Malaysia, pp. 87–132.
- Othman, A.S., Ghani, A.A., Roslee, K.H., 2000. Field relations and petrochemistry of the Jeli igneous complex, north Kelantan: preliminary observations. *Proceedings, Geological Society of Malaysia Annual Conference 2000*, 105–110.
- Prosser, S., 1993. Rift-related linked depositional systems and their seismic expression. *Geol. Soc. Spec. Publ.* 71, 35–66.
- Pubellier, M., Morley, C.K., 2014. The basins of Sundaland (SE Asia): evolution and boundary conditions. *Mar. Pet. Geol.* 58 (Part B), 555–578.
- Ranalli, G., Brown, R.L., Boschadin, R., 1989. A geodynamic model for extension in the Shuswap core complex, southeastern Canadian Cordillera. *Can. J. Earth Sci.* 26, 1647–1653.
- Ridd, M.F., 2012. The role of strike-slip faults in the displacement of the Palaeotethys suture zone in Southeast Thailand. *J. Asian Earth Sci.* 51, 63–84.
- Ridd, M.F., 2013. A middle permian-middle Triassic accretionary complex and a late triassic Foredeep basin: forerunners of an Indosinian (Late Triassic) thrust complex in the Thailand-Malaysia border area. *J. Asian Earth Sci.* 76, 99–114.
- Rutter, E.H., Elliott, D., 1976. The kinetics of rock deformation by pressure solution [and discussion]. *Philos. Trans. R. Soc. London, Ser. A, Math. Phys. Sci.* 283, 203–219.
- Ryall, P.J.C., 1982. Some thoughts on the crustal structure of Peninsular Malaysia - results of gravity traverse. *Bull. Geol. Soc. Malaysia* 15, 9–18.
- Searle, M.P., Whitehouse, M.J., Robb, L.J., Ghani, A.A., Hutchison, C.S., Sone, M., Ng, S.W.P., Roselee, M.H., Chung, S.L., Oliver, G.J.H., 2012. Tectonic evolution of the Sibumasu-Indochina terrane collision zone in Thailand and Malaysia: constraints from new U-Pb zircon chronology of SE Asian tin granitoids. *J. Geol. Soc.* 169, 489–500.
- Setiawan, Jatmika, Abdullah, Ibrahim, 2003. The structure and deformation history of the serpentinite bodies along the Bentong Suture: a case study at Bukit Rokan Barat. *Geol. Soc. Malaysia Bull.* 46, 329–334.
- Sevastjanova, I., Hall, R., Alderton, D., 2012. A detrital heavy mineral viewpoint on sediment provenance and tropical weathering in SE Asia. *Sed. Geol.* 280, 179–194.
- Singh, D.S., Chu, L.H., Teoh, L.H., Loganathan, P., Cobbing, E.J., Mallick, D.I.J., 1984. The Stong complex: a reassessment. *Bull. Geol. Soc. Malaysia* 17, 61–77.
- Sonder, L.J., England, P.C., 1989. Effects of temperature-dependent rheology on large-scale continental extension. *J. Geophys. Res.* 94, 7603–7619.
- Sone, M., Metcalfe, I., 2008. Parallel Tethyan sutures in mainland Southeast Asia: new insights for Palaeo-Tethys closure and implications for the Indosinian orogeny. *C.R. Geosci.* 340, 166–179.
- Spencer, J.E., 1984. Role of tectonic denudation in warping and uplift of low-angle normal faults. *Geology* 12, 95–98.
- Stojadinovic, U., Matenco, L., Andriessen, P.A.M., Toljić, M., Foeken, J.P.T., 2013. The balance between orogenic building and subsequent extension during the Tertiary evolution of the NE Dinarides: constraints from low-temperature thermochronology. *Global Planet. Change* 103, 19–38.
- Tan, B.K., 1984. The tectonic framework and evolution of the central belt and its margins, Peninsular Malaysia. *Bull. Geol. Soc. Malaysia* 17, 307–322.
- Tan, B.K., 1996. 'Suture zones' in peninsular Malaysia and Thailand: implications for palaeotectonic reconstruction of southeast Asia. *J. SE Asian Earth Sci.* 13, 243–249.
- Tan, B.K., Khoo, T.T., 1993. Clinopyroxene composition and tectonic setting of the Bentong-Raub belt, Peninsular Malaysia. *J. SE Asian Earth Sci.* 8, 539–545.
- Tate, R.B., Tan, D.N.K., Ng, T.F., 2008. *Geological Map of Peninsular Malaysia. Scale 1:1,000,000*. Geological Society of Malaysia, Kuala Lumpur, Malaysia.
- Tirel, C., Brun, J.P., Burov, E., 2004. Thermomechanical modeling of extensional gneiss domes. In: Whitney, D.L., Teyssier, C., Siddoway, C.S. (Eds.), *Gneiss Domes in Orogeny*. Geological Society of America Special Paper 380, Boulder, Colorado, pp. 67–78.
- Tjia, H.D., 1969. Regional implication of Lebir fault zone. *Geol. Soc. Malaysia Newsletter* 19, 6–7.
- Tjia, H.D., 1984. Multi-directional tectonic movements in the schist of Bentong, Pahang. *Bull. Geol. Soc. Malaysia* 10, 187–190.
- Tjia, H.D., 1987. Olistostrome in the Bentong area, Pahang. *Warta Geol.* 13, 105–111.
- Tjia, H.D., 1994. Inversion tectonics in the Malay Basin: evidence and timing of events. *Bull. Geol. Soc. Malaysia* 56, 119–126.
- Tjia, H.D., 1996. Tectonics of deformed and undeformed Jurassic-Cretaceous strata of Peninsular Malaysia. *Bull. Geol. Soc. Malaysia* 39, 131–156.
- Tjia, H.D., 1998. Meridian-parallel faults and Tertiary basins of Sundaland. *Bull. Geol. Soc. Malaysia* 42, 101–118.
- Tjia, H.D., Slnanshoor, Syed Sheikh, 1996. The Bentong suture in southwest Kelantan, Peninsular Malaysia. *Bull. Geol. Soc. Malaysia* 39, 195–211.
- Tulot, S., Umor, M.R., 2001. Asalan xenolit di dalam pluton Granit Noring, Kompleks Stong, Kelantan (Origin of xenoliths in Noring granite pluton, Stong Complex, Kelantan). *Proceedings, Geological Society of Malaysia Annual Conference 2001*, 155–160.
- Umor, M.R., Ghani, A.A., Mohamad, H., 2001. Pembahagian unit batuan di dalam Pluton Berangkat, Kompleks Stong, Jeli Kelantan berdasarkan kajian lapangan, petrogra dan geokimia batuan. *Bull. Geol. Soc. Malaysia* 58, 49–54.
- Umor, M.R., Ghani, A.A., Mohamad, H., Heng, G.S., 2006. Geochemistry of the Stong igneous complex. In: *Proceedings, 2nd Symposium of the International Geologic Correlation Programme (Project 516) Geological Anatomy of East and South Asia*, pp. 75–76.
- Umor, M.R., Ghani, A.A., Mohamad, H., 2012. Volcanic rocks of the Semantan formation in the vicinity of Gunung Benom, Pahang. *Bull. Geol. Soc. Malaysia* 58, 43–48.
- Vermeesch, P., 2009. RadialPlotter: a java application for fission track, luminescence and other radial plots. *Radiat. Meas.* 44, 409–410.
- Visser, R.L.M., 2012. Extension in a convergent tectonic setting: a lithospheric view on the Alboran system of SW Europe. *Geologica Belgica* 15, 53–72.
- Wernicke, B., 1985. Uniform-sense normal simple shear of the continental lithosphere. *Can. J. Earth Sci.* 22, 108–125.
- Wernicke, B., 1992. Cenozoic extensional tectonics of the U.S. Cordillera. In: B.C., B., Lipman, P.W., Zoback, M.L. (Eds.), *The Cordilleran orogen: Conterminous U.S.: Boulder, Colorado, Geological Society of America*, pp. 553–581.
- Wernicke, B., Axen, G.J., 1988. On the role of isostasy in the evolution of normal fault systems. *Geology* 848–851.
- Yin, E.H., 1965. Provisional Draft Report on the Geology and Mineral Resources of the Gua Musang Area, Sheet 45. Geological Survey of Malaysia, South Kelantan, Kuala Lumpur.
- Ziegler, P.A., Cloetingh, S., 2004. Dynamic processes controlling evolution of rifted basins. *Earth Sci. Rev.* 64, 1–50.
- Ziegler, P.A., Cloetingh, S., van Wees, J.-D., 1995. Dynamics of intra-plate compressional deformation: the Alpine foreland and other examples. *Tectonophysics* 252, 7–22.